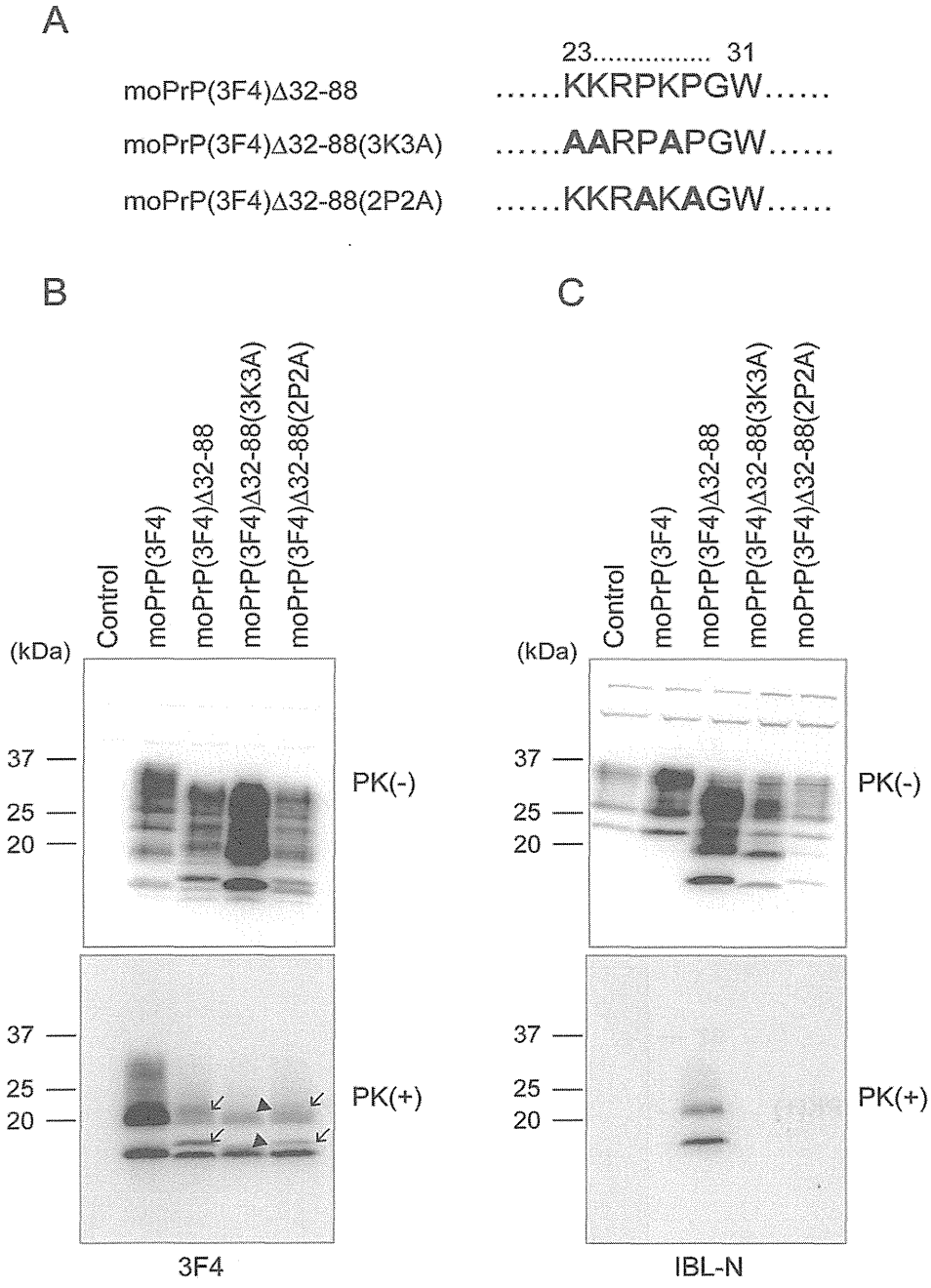

Figure 6. Lysine residues are important for the pre-OR residues 23–31 to form a PK-resistant structure in prion-infected N2a cells. (A) Amino acid sequences of the pre-OR residues 23–31 in moPrP(3F4) Δ32–88, moPrP(3F4) Δ32–88(3K3A) and moPrP(3F4) Δ32–88(2P2A). Bold residues indicate substituted alanine residues. (B) Western blotting of N2aC24L1-3 cells transfected with control pcDNA3.1(+) and expression vectors encoding moPrP(3F4), moPrP(3F4) Δ32–88, moPrP(3F4) Δ32–88(3K3A) and moPrP(3F4) Δ32–88(2P2A) using 3F4 anti-PrP antibodies. The cell lysates were treated with PK at 5 μg/ml. All mutant proteins were converted into PK-resistant isoforms in N2aC24L1-3 cells. The PK treatment revealed doublet non-glycosylated and mono-glycosylated bands in moPrP(3F4)^{Sc}Δ32–88 (arrows), indicating that the pre-OR region of some moPrP(3F4)^{Sc}Δ32–88 molecules is PK-resistant. Similar doublet bands were observed in moPrP(3F4)^{Sc}Δ32–88(2P2A) (arrows). However, moPrP(3F4)^{Sc}Δ32–88(3K3A) gave rise to doublet bands with the upper band migrating very closely to the lower band (arrowheads). (C) Since substitution of proline residues into alanine residues disrupted the IBL-N epitope, the PK-resistant pre-OR residues in moPrP(3F4)^{Sc}Δ32–88(2P2A) failed to be visualized by IBL-N anti-PrP antibodies.
doi:10.1371/journal.pone.0043540.g006

levels of PrP^{Sc}Δ32–93 and prion infectivity are lower in tg(PrPΔ32–93)/*Prnp*$^{0/0}$ mice [9]. Astrogliosis was easily detectable in the brains of tg(PrPΔOR)/*Prnp*$^{0/0}$ mice, but undetectable in tg(PrPΔ32–93)/*Prnp*$^{0/0}$ mice [9]. The foreleg paresis was developed at early stages in tg(PrPΔOR)/*Prnp*$^{0/0}$ mice, but only at late stages in tg(PrPΔ32–93)/*Prnp*$^{0/0}$ mice [9]. These results

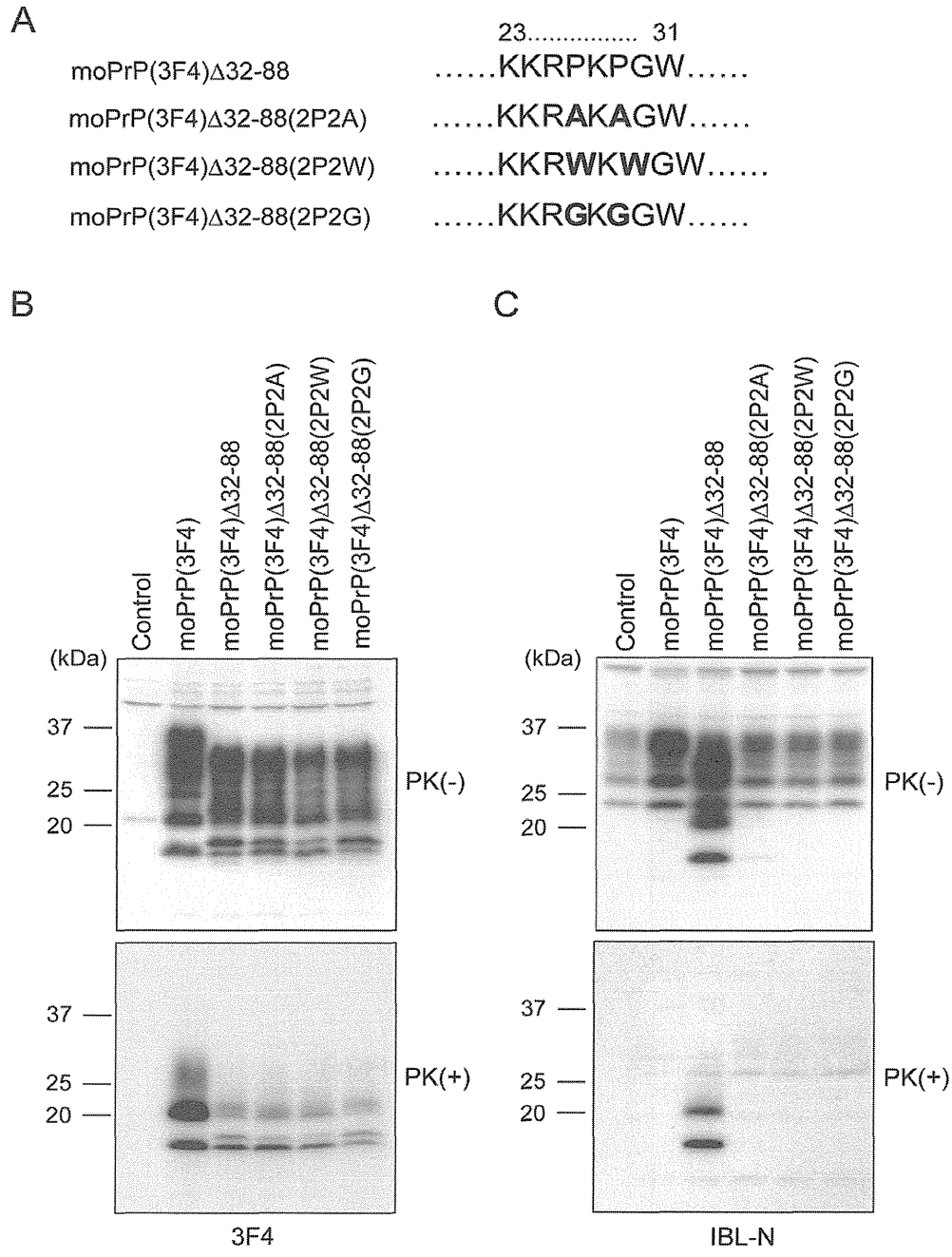

Figure 7. The pre-OR residues 23–31 with a substitution of the proline residues by tryptophan or glycine residues form a PK-resistant structure in prion-infected N2a cells. (A) Amino acid sequences of the pre-OR residues 23–31 in mutant proteins. Bold residues indicate substituted residues. (B) Western blotting of N2aC24L1-3 cells transfected with control pcDNA3.1(+) and expression vectors encoding each mutant protein using 3F4 anti-PrP antibodies. The cell lysates were treated with PK at 5 μg/ml. All of the mutant proteins were converted into PK-resistant isoforms in N2aC24L1-3 cells, and all of the mutant isoforms, moPrP(3F4)^{Sc}Δ32–88, moPrP(3F4)^{Sc}Δ32–88(2P2A), moPrP(3F4)^{Sc}Δ32–88(2P2W) and moPrP(3F4)^{Sc}Δ32–88(2P2G), gave rise to similar doublet non-glycosylated and mono-glycosylated bands. (C) Since substitution of proline residues into alanine, tryptophan or glycine residues disrupted the IBL-N epitope, the PK-resistant pre-OR residues in these mutant proteins failed to be visualized by IBL-N anti-PrP antibodies.
doi:10.1371/journal.pone.0043540.g007

suggest that the effects of deletion of the OR region alone on conversion are limited, compared to those of deletion of residues 32–93 including the OR region. Therefore, the levels of PK-resistant PrP and prion infectivity were higher in the brains of tg(PrPΔOR)/*Prnp*$^{0/0}$ mice than in tg(PrPΔ32–93)/*Prnp*$^{0/0}$ mice. Consequently, astrogliosis was detectable in tg(PrPΔOR)/*Prnp*$^{0/0}$ mice but not in tg(PrPΔ32–93)/*Prnp*$^{0/0}$ mice. The onset of foreleg paresis could be associated with the amounts of PrP^{Sc}ΔOR or PrP^{Sc}Δ32–93 in the brain or in the spinal cord. However, the exact mechanism underlying the foreleg paresis remains unknown.

A

	23..... 31
moPrP(3F4)Δ32-88	.....KKRPKPGW.....
moPrP(3F4)Δ32-88(3K3A)	.....AARPAPGW.....
moPrP(3F4)Δ32-88(K23A)	.....AKRPKPGW.....
moPrP(3F4)Δ32-88(K24A)	.....KARPKPGW.....
moPrP(3F4)Δ32-88(K27A)	.....KKRPAPGW.....
moPrP(3F4)Δ32-88(K23,24A)	.....AARPKPGW.....
moPrP(3F4)Δ32-88(K23,27A)	.....AKRPAPGW.....
moPrP(3F4)Δ32-88(K24,27A)	.....KARPAPGW.....
moPrP(3F4)Δ32-88(3K3R)	.....RRRPRPGW.....

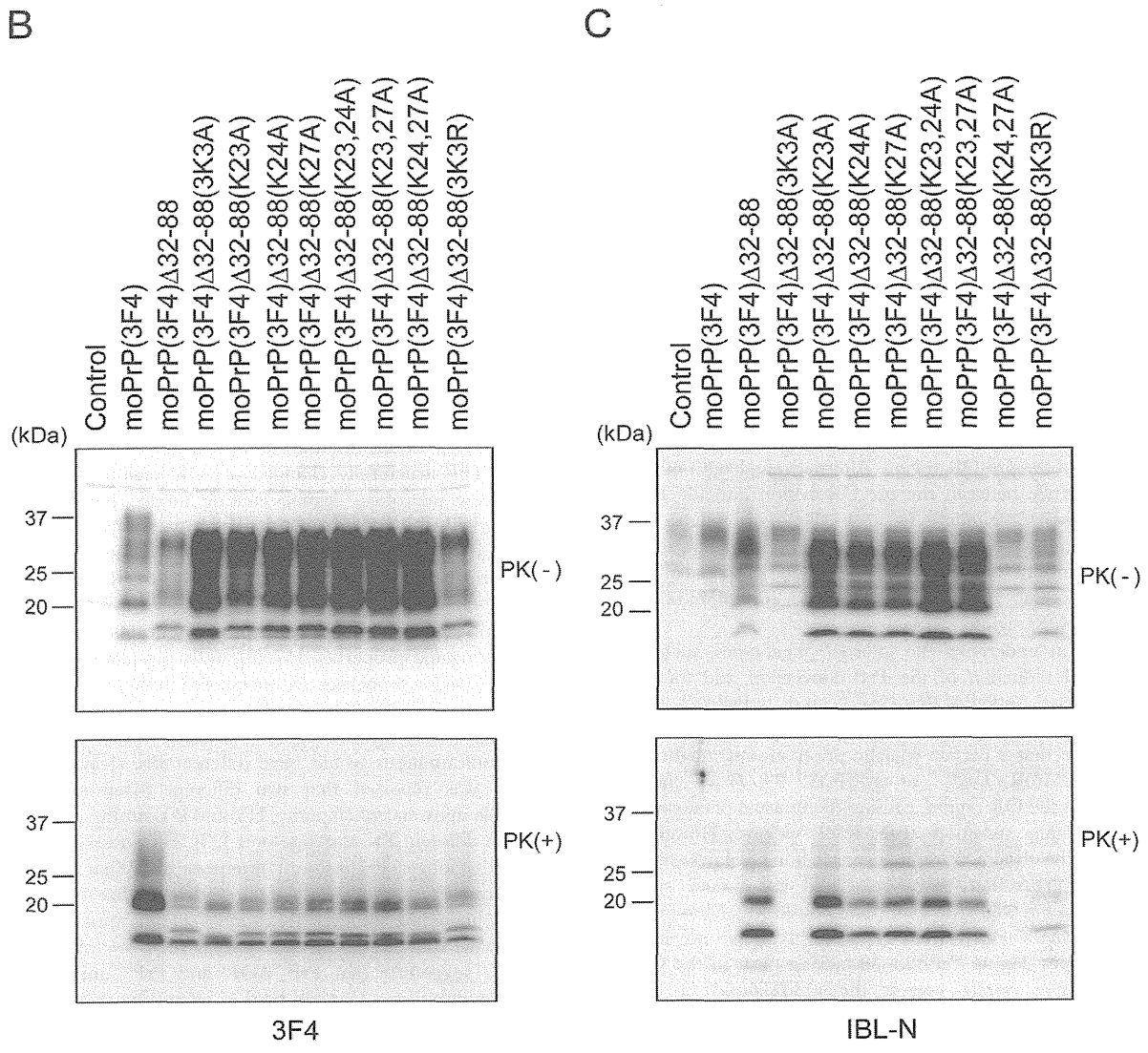

Figure 8. Positively charged lysine residues, particularly located at codons 24 and 27, are importnat for the pre-OR residues 23–31 to form a PK-resistant structure in prion-infected N2a cells. (A) Amino acid sequences of the pre-OR residues 23–31 in mutant proteins. Bold residues indicate substituted residues. (B) Western blotting of N2aC24L1-3 cells transfected with control pcDNA3.1(+) and expression vectors encoding each mutant protein using 3F4 anti-PrP antibodies. The cell lysates were treated with PK at 5 μg/ml. All of the mutant proteins were converted into PK-resistant isoforms in N2aC24L1-3 cells, and all of the mutant isoforms gave rise to doublet non-glycosylated and mono-glycosylated bands. The doublet bands of moPrP(3F4)^{Sc}Δ32–88(K23A), moPrP(3F4)^{Sc}Δ32–88(K24A) and moPrP(3F4)^{Sc}Δ32–88(K27A) were similar in molecular size to those of moPrP(3F4)^{Sc}Δ32–88. However, moPrP(3F4)^{Sc}Δ32–88(K24,27A) gave rise to the doublet band with the upper band migrating very closely to the lower band, similarly to moPrP(3F4)^{Sc}Δ32–88(3K3A). MoPrP(3F4)^{Sc}Δ32–88(K23,24A) and moPrP(3F4)^{Sc}Δ32–88(K23,27A) showed the upper band with an intermediate molecular size. MoPrP(3F4)^{Sc}Δ32–88(3K3R) giving rise to doublet bands with similar molecular size to those of moPrP(3F4)^{Sc}Δ32–88. (C) IBL-N antibodies recognized all of the PK-resistant isoforms except for moPrP(3F4)^{Sc}Δ32–88(3K3A) and moPrP(3F4)^{Sc}Δ32–88(K24,27A).
doi:10.1371/journal.pone.0043540.g008

Upon the conversion of PrP^{C} into PrP^{Sc}, only the 2/3 C-terminal part of PrP^{C} undergoes profound conformational changes to form the PK-resistant core of PrP^{Sc} [1]. In contrast, the N-terminal part of PrP^{Sc} remains PK-sensitive [1]. Consistent with this, we failed to detect any PK-resistant fragments with molecular size >2 kDa in the brains of terminally ill wild-type mice on Western blotting with IBL-N anti-N-terminus antibodies (data not shown). However, we found here that the entire PrP^{Sc}ΔOR, including the pre-OR residues 23–50, appeared unusually PK-resistant. No data were available whether the pre-OR region of PrP^{Sc}Δ32–93 were PK-resistant [9]. However, it is very likely that the region could be PK-resistant in PrP^{Sc}Δ32–93 because the OR region was completely deleted in PrPΔ32–93. Indeed, we found that the entire PrPΔ32–88, including the pre-OR residues 23–31, was converted to be PK-resistant in infected N2a cells. These results indicate that the pre-OR region has a potential to undergo conformational changes to become PK-resistant upon conversion, and that the OR region usually prevents the pre-OR region from undergoing such conformational changes. We also showed that the conversion activity of the pre-OR region in PrPΔ32–88 was diminished by substitution of either all of the positively charged lysine residues or of lysine residues 24 and 27 with uncharged alanine residues, but not affected by a substitution of all the lysine residues with positively charged arginine residues. These results suggest that the positive charge at 24 and 27 residues might be important for the pre-OR region to form a PK-resistant structure when the OR region is deleted. Deletion of the authentic PK cleavage site located within the OR region might be relevant to the unusual folding of the pre-OR region. Alternatively, length of the intervening sequence between the pre-OR region and the PK-resistant C-terminal core might be a key factor to induce the unusual folding in the pre-OR region. It is also possible that, since the OR region binds to Cu^{2+} via a histidine residue [17], loss of the binding activity to Cu^{2+} might be responsible for formation of the PK-resistant pre-OR region.

The mechanism underlying the unusual phenotypes, such as brain-preferential reduction of the PrP conversion and foreleg paresis, in infected tg(PrPΔOR)/$Prnp^{0/0}$ and tg(PrPΔ32–93)/$Prnp^{0/0}$ mice remains unknown. RML prions are a strain mixture. It is thus possible that a certain specific prion strain(s) might be selected in tg(PrPΔOR)/$Prnp^{0/0}$ or tg(PrPΔ32–93)/$Prnp^{0/0}$ mice because of lack of the OR region, causing the unusual phenotypes in these mice after infection with RML prions. However, inoculation of the brain or spinal cord homogenates from terminally ill tg(PrPΔOR)/$Prnp^{0/0}$ mice did not induce such unusual phenotypes in wild-type mice (data not shown). Moreover, tg(PrPΔ23–88)/$Prnp^{0/0}$ mice were reported to show no such unusual phenotypes despite PrPΔ23–88 lacking most of the OR region [10]. These results suggest the unlikelihood of this possibility. Another possibility is that the overexpression of PrPΔOR or PrPΔ32–93 in the spinal cords might cause high accumulation of PrP^{Sc}ΔOR in the spinal cords, resulting in development of the unusual phenotypes in these infected mice. However, PrP^{Sc}ΔOR was accumulated in the spinal cords of infected tg(PrPΔOR)/$Prnp^{0/0}$ mice at a similar level to that of wild-type PrP^{Sc} in infected wild-type mice. Moreover, no foreleg paresis was reported in infected tg(PrPΔ23–88)/$Prnp^{0/0}$ and tg(moPrP)/$Prnp^{0/0}$ mice [10]. Tg(PrPΔ23–88) and tg(moPrP) mice were generated using the same cos.SHaTet expression vector system as in tg(PrPΔOR) mice [10,12], indicating that, similarly to PrPΔOR in tg(PrPΔOR)/$Prnp^{0/0}$ mice, PrPΔ23–88 and $moPrP^{C}$ are overexpressed in the brains and spinal cords of these mice. Therefore, this possibility is also unlikely. Alternatively, the unusual phenotypes in infected tg(PrPΔOR)/$Prnp^{0/0}$ or tg(PrPΔ32–93)/$Prnp^{0/0}$ mice might be due to indirect effects caused by deletion of the OR region, but not due to direct effects of deletion of the OR region. PrPΔOR and PrPΔ32–93 include the pre-OR residues 23–31 intact, whereas PrPΔ23–88 does not, suggesting that the pre-OR residues in PrP^{Sc}ΔOR and PrP^{Sc}Δ32–93 might be associated with the unusual phenotypes in tg(PrPΔOR)/$Prnp^{0/0}$ and tg(PrPΔ32–93)/$Prnp^{0/0}$ mice. Indeed, we showed here that the pre-OR residues of PrP^{Sc}ΔOR or possibly PrP^{Sc}Δ32–93 were unusually PK-resistant. The pre-OR region binds to glycosaminoglycans, the polysaccharide chains of proteoglycans, via the positively charged lysine-rich region [18], and the binding of PrP to glycosaminoglycans is important for conversion [19]. Therefore, the structurally changed pre-OR region in PrP^{Sc}ΔOR and PrP^{Sc}Δ32–93 might alter the binding affinity to a yet unidentified proteoglycan(s) important for conversion in the brain, resulting in disturbance of conversion in the brain. The structurally changed pre-OR region also might induce a new neurotoxic signal, causing foreleg paresis as in infected tg(PrPΔOR)/$Prnp^{0/0}$ or tg(PrPΔ32–93)/$Prnp^{0/0}$ mice. However, further studies are required to elucidate the mechanism of the unusual phenotypes in infected tg(PrPΔOR)/$Prnp^{0/0}$ or tg(PrPΔ32–93)/$Prnp^{0/0}$ mice.

There are many different groups of prion strains with strain-specific pathogenic properties [17,20]. It is postulated that the prion strain-specific properties are enciphered in the strain-specific conformation of PrP^{Sc} [21,22]. Since changes in the protein conformation would cause changes in PK-accessibility, PrP^{Sc}s with different conformations would have different PK cleavage sites. Indeed, it was reported that two different prion strains of transmissible mink encephalopathy, HY and DY strains, produced PrP^{Sc}s with different PK cleavage sites [23]. HY strain produced PrP^{Sc} with a longer PK-resistant fragment than that of PrP^{Sc} produced by DY strain [24]. We showed here that the entire PrP^{Sc}ΔOR, including the pre-OR residues 23–50, appeared PK-resistant, while only the C-terminal part is PK-resistant in wild-type PrP^{Sc}, suggesting that PrP^{Sc}ΔOR and PrP^{Sc} might form different conformations. It might be thus interesting to characterize the biological properties of prions associated with PrP^{Sc}ΔOR.

Supporting Information

Figure S1 Similar spongiform change in the brains of infected wild-type and tg(PrPΔOR)/*Prnp*$^{0/0}$ mice. The brains of uninfected or terminally ill wild-type and tg(PrPΔOR)/*Prnp*$^{0/0}$ mice were subjected to HE staining. Vacuoles were scant in the cerebral cortex (A) but common in the hippocampus (B), and cerebellum (C). No specific vacuoles were observed in the brains of uninfected mice.
(TIF)

Figure S2 Similar distribution of PrP^{Sc} and PrP^{Sc}ΔOR in the brains of infected wild-type and tg(PrPΔOR)/*Prnp*$^{0/0}$ mice. The brains of uninfected or terminally ill wild-type and tg(PrPΔOR)/*Prnp*$^{0/0}$ mice were subjected to immunohistochemistry with IBL-N anti-PrP antibodies after treatment with formic acid. The immunoreactive signals were similarly observed in the brains of both types of infected mice, but not in control uninfected mice. (A), cerebral cortex; (B), hippocampus; (C), cerebellum.
(TIF)

Table S1 Primers used in the present study.
(DOC)

Acknowledgments

We thank Stanley B. Prusiner for providing Zrch I *Prnp*$^{0/0}$ mice

Author Contributions

Conceived and designed the experiments: SS SK. Performed the experiments: YY HM KU AO SI TM NM. Analyzed the data: SS HM. Wrote the paper: SS.

References

1. Prusiner SB (1998) Prions. Proc Natl Acad Sci U S A 95: 13363–13383.
2. Weissmann C, Enari M, Klohn PC, Rossi D, Flechsig E (2002) Molecular biology of prions. Acta Neurobiol Exp (Wars) 62: 153–166.
3. Prusiner SB (1982) Novel proteinaceous infectious particles cause scrapie. Science 216: 136–144.
4. Bueler H, Aguzzi A, Sailer A, Greiner RA, Autenried P, et al. (1993) Mice devoid of PrP are resistant to scrapie. Cell 73: 1339–1347.
5. Prusiner SB, Groth D, Serban A, Koehler R, Foster D, et al. (1993) Ablation of the prion protein (PrP) gene in mice prevents scrapie and facilitates production of anti-PrP antibodies. Proc Natl Acad Sci U S A 90: 10608–10612.
6. Manson JC, Clarke AR, McBride PA, McConnell I, Hope J (1994) PrP gene dosage determines the timing but not the final intensity or distribution of lesions in scrapie pathology. Neurodegeneration 3: 331–340.
7. Sakaguchi S, Katamine S, Shigematsu K, Nakatani A, Moriuchi R, et al. (1995) Accumulation of proteinase K-resistant prion protein (PrP) is restricted by the expression level of normal PrP in mice inoculated with a mouse-adapted strain of the Creutzfeldt-Jakob disease agent. J Virol 69: 7586–7592.
8. Stahl N, Borchelt DR, Hsiao K, Prusiner SB (1987) Scrapie prion protein contains a phosphatidylinositol glycolipid. Cell 51: 229–240.
9. Flechsig E, Shmerling D, Hegyi I, Raeber AJ, Fischer M, et al. (2000) Prion protein devoid of the octapeptide repeat region restores susceptibility to scrapie in PrP knockout mice. Neuron 27: 399–408.
10. Supattapone S, Muramoto T, Legname G, Mehlhorn I, Cohen FE, et al. (2001) Identification of two prion protein regions that modify scrapie incubation time. J Virol 75: 1408–1413.
11. Supattapone S, Bosque P, Muramoto T, Wille H, Aagaard C, et al. (1999) Prion protein of 106 residues creates an artifical transmission barrier for prion replication in transgenic mice. Cell 96: 869–878.
12. Yoshikawa D, Yamaguchi N, Ishibashi D, Yamanaka H, Okimura N, et al. (2008) Dominant-negative effects of the N-terminal half of prion protein on neurotoxicity of prion protein-like protein/doppel in mice. J Biol Chem 283: 24202–24211.
13. Fujita K, Yamaguchi Y, Mori T, Muramatsu N, Miyamoto T, et al. (2011) Effects of a Brain-Engraftable Microglial Cell Line Expressing Anti-Prion scFv Antibodies on Survival Times of Mice Infected with Scrapie Prions. Cellular and Molecular Neurobiology 31: 999–1008.
14. Reed J, Muench H (1938) A simple method of estimating fifty per cent endpoints. American Journal of Hygiene 27: 493–497.
15. Weissmann C, Flechsig E (2003) PrP knock-out and PrP transgenic mice in prion research. British Medical Bulletin 66: 43–60.
16. Fischer M, Rulicke T, Raeber A, Sailer A, Moser M, et al. (1996) Prion protein (PrP) with amino-proximal deletions restoring susceptibility of PrP knockout mice to scrapie. Embo J 15: 1255–1264.
17. Brown DR, Qin K, Herms JW, Madlung A, Manson J, et al. (1997) The cellular prion protein binds copper in vivo. Nature 390: 684–687.
18. Warner RG, Hundt C, Weiss S, Turnbull JE (2002) Identification of the heparan sulfate binding sites in the cellular prion protein. J Biol Chem 277: 18421–18430.
19. Priola SA, Caughey B (1994) Inhibition of scrapie-associated PrP accumulation. Probing the role of glycosaminoglycans in amyloidogenesis. Mol Neurobiol 8: 113–120.
20. Bruce ME, Fraser H (1991) Scrapie strain variation and its implications. Current topics in Microbiology and Immunology 172: 125–138.
21. Chien P, Weissman JS (2001) Conformational diversity in a yeast prion dictates its seeding specificity. Nature 410: 223–227.
22. Gambetti P, Cali I, Notari S, Kong Q, Zou WQ, et al. (2011) Molecular biology and pathology of prion strains in sporadic human prion diseases. Acta neuropathologica 121: 79–90.
23. Bessen RA, Marsh RF (1992) Biochemical and physical properties of the prion protein from two strains of the transmissible mink encephalopathy agent. Journal of Virology 66: 2096–2101.
24. Bessen RA, Marsh RF (1994) Distinct PrP properties suggest the molecular basis of strain variation in transmissible mink encephalopathy. Journal of Virology 68: 7859–7868.

THE JOURNAL OF BIOLOGICAL CHEMISTRY VOL. 287, NO. 17, pp. 14023–14039, April 20, 2012

Direct Evidence of Generation and Accumulation of β-Sheet-rich Prion Protein in Scrapie-infected Neuroblastoma Cells with Human IgG1 Antibody Specific for β-Form Prion Protein*[S]

Received for publication, October 28, 2011, and in revised form, February 17, 2012 Published, JBC Papers in Press, February 22, 2012, DOI 10.1074/jbc.M111.318352

Toshiya Kubota[‡], Yuta Hamazoe[‡], Shuhei Hashiguchi[‡], Daisuke Ishibashi[§], Kazuyuki Akasaka[¶], Noriyuki Nishida[§], Shigeru Katamine[§], Suehiro Sakaguchi[‖], Ryota Kuroki[**], Toshihiro Nakashima[‡‡], and Kazuhisa Sugimura[‡1]

From the [‡]Department of Chemistry, Biotechnology, and Chemical Engineering, Graduate School of Science and Engineering, Kagoshima University, Kagoshima 890-0065, Japan, [¶]Department of Biotechnological Science, School of Biology-oriented Science and Technology, Kinki University, 930 Nishimitani, Kinokawa-shi, Wakayama 649-6493, Japan, [§]Department of Molecular Microbiology and Immunology, Graduate School of Biomedical Science, Nagasaki University, 1-12-4 Sakamoto, Nagasaki 852-8523, Japan, [‖]Division of Molecular Neurobiology, The Institute for Enzyme Research, The University of Tokushima, Kuramoto-cho 3-18-15, Tokushima 770-8503, Japan, [**]Neutron Science Research Center, Japan Atomic Energy Research Institute, 2-4 Shirane Shirakata, Tokai, Naka-gun, Ibaraki 319-1195, Japan, and [‡‡]The Chemo-Sero-Therapeutic Research Institute, Kyokushi Kikuchi, Kumamoto 869-1298, Japan

Background: PrP^{Sc} is believed to have a β-sheet-rich structure.
Results: Established human IgG1 stained β-form PrP in prion-infected cells but had no inhibitory activity against the propagation of PrP^{res}.
Conclusion: β-Sheet-rich PrP was generated and accumulated in cells.
Significance: β-Form PrP aggregates play roles in cytotoxicity, whereas prion or PrP^{Sc} is responsible for prion propagation.

We prepared β-sheet-rich recombinant full-length prion protein (β-form PrP) (Jackson, G. S., Hosszu, L. L., Power, A., Hill, A. F., Kenney, J., Saibil, H., Craven, C. J., Waltho, J. P., Clarke, A. R., and Collinge, J. (1999) *Science* 283, 1935–1937). Using this β-form PrP and a human single chain Fv-displaying phage library, we have established a human IgG1 antibody specific to β-form but not α-form PrP, PRB7 IgG. When prion-infected ScN2a cells were cultured with PRB7 IgG, they generated and accumulated PRB7-binding granules in the cytoplasm with time, consequently becoming apoptotic cells bearing very large PRB7-bound aggregates. The SAF32 antibody recognizing the N-terminal octarepeat region of full-length PrP stained distinct granules in these cells as determined by confocal laser microscopy observation. When the accumulation of proteinase K-resistant PrP was examined in prion-infected ScN2a cells cultured in the presence of PRB7 IgG or SAF32, it was strongly inhibited by SAF32 but not at all by PRB7 IgG. Thus, we demonstrated direct evidence of the generation and accumulation of β-sheet-rich PrP in ScN2a cells *de novo*. These results suggest first that PRB7-bound PrP is not responsible for the accumulation of β-form PrP aggregates, which are rather an end product resulting in the triggering of apoptotic cell death, and second that SAF32-bound PrP lacking the PRB7-recognizing β-form may represent so-called PrP^{Sc} with prion propagation activity. PRB7 is the first human antibody specific to β-form PrP and has become a powerful tool for the characterization of the biochemical nature of prion and its pathology.

Prion diseases are fatal and transmissible neurodegenerative disorders that include Creutzfeldt-Jakob disease in humans and bovine spongiform encephalopathy in cattle. It has been proposed that a misfolded form of prion protein is responsible for the infectivity of prion disease, and the pathogenesis of prion disease involves a conformational change of prion protein (PrP)[2] from PrP^{C} to PrP^{Sc} (1). PrP^{C} is a monomeric isoform, rich in α-helical structure, and sensitive to digestion by proteinase K (PK). In contrast, multimers are PrP^{Sc} characterized as PrP^{res} by enhanced resistance toward PK digestion. Consequently, it is believed first that PrP^{Sc} might have a β-pleated sheet structure because all amyloids studied have been found to have this structure and second that this β-sheet-rich PrP^{Sc}

* This work was supported by Grants-in-aid for Scientific Research C 16613008 and for Young Scientists B 22790435 from the Ministry of Education, Culture, Sports, Science and Technology of Japan (to S. H.), Health and Labour Sciences Research Grants on Food Safety (Shokuhin-016) (to S. H.) and Psychiatric and Neurological Diseases and Mental Health from the Ministry of Health, Labour and Welfare (to S. H. and K. S.), a grant-in-aid from the Bovine Spongiform Encephalopathy Control Project of the Ministry of Agriculture, Forestry and Fisheries of Japan (to K. S.), and Super Special Consortia for supporting the development of cutting-edge medical care from 2008 to 2012 (to K. S.).
[S] This article contains supplemental Figs. S1–S7.
[1] To whom correspondence should be addressed: Dept. of Chemistry, Biotechnology, and Chemical Engineering, Graduate School of Science and Engineering, Kagoshima University, Kagoshima 1-21-40 Korimoto, Kagoshima 890-0065, Japan. Tel.: 81-99-285-8345; Fax: 81-99-258-4706; E-mail: kazu@be.kagoshima-u.ac.jp.

[2] The abbreviations used are: PrP, prion protein; PK, proteinase K; VhIs, heavy-chain leader sequence; Vh, heavy-chain variable gene; Vl, light-chain variable gene; VlIs, light-chain leader sequence; scFv, single chain Fv(s); IGHC1, human immunoglobulin heavy chain 1; IGKC, human immunoglobulin κ-chain; ScN2a, Scrapie-infected neuroblastoma; rPrP, recombinant full-length prion protein; GdnHCl, guanidine hydrochloride; Tricine, *N*-[2-hydroxy-1,1-bis(hydroxymethyl)ethyl]glycine; SEC, size exclusion chromatography.

binds specifically to PrP^{C}, propagating its altered conformation via a templating mechanism, which is a prion activity. In other words, it was demonstrated that PrP^{Sc}, defined as PrP27–30, was generated and accumulated in prion-infected cells or brain. However, there is no direct evidence of whether prion or PrP^{Sc} has a β-sheet-rich structure, although there is suggestive evidence of FTIR using centrifugation-purified aggregates of prion-infected brain extracts (2, 3).

Antibodies to these proteins are powerful tools to clarify these questions. However, 1) the purification procedure of PrP^{Sc} was based on the centrifugation precipitation of molecular aggregates using PEG or sodium phosphotungstic acid, which does not necessarily guarantee the specificity to a prion (2, 4–7). 2) The specificity of an anti-PrP^{Sc} antibody was defined by the existence of PrP27–30 resulting from PK-treated prion-infected brain or cell extracts that are immunoprecipitated with tested antibodies. These experiments showed that PrP27–30 was resolved from PK-resistant PrP but do not directly indicate that PrP27–30 is generated from β-sheet-rich PrP; *i.e.* they rather suggest a generation of β-sheet-rich PrP by experimental procedures including the use of PK, denaturing agents, or detergents (8). 3) All antibodies established so far are either anti-PrP^{Sc}/PrP^{C} or anti-PrP^{C} antibodies (9). More recently, mouse monoclonal IgG W261, which reacts exclusively with PrP^{Sc} but not PrP^{C}, has been reported by cell fusion technology using spleen cells immunized with sodium phosphotungstic acid-precipitated PrP^{Sc} derived from prion-infected brain extracts (10). This study did not address the question of whether PrP^{Sc} was the β-form PrP or not.

In this study, using the conformation-defined recombinant PrPs and a human single chain Fv-displaying phage library, we have established two human IgG, PRB7 and PRB30, which are specific to the β-form but not the α-form of recombinant PrP of human, bovine, sheep, and mouse. Epitope mapping analysis showed that PRB7 IgG recognized residues 128–132 of the full-length prion protein.

When prion-infected ScN2a cells were cultured in the presence of PRB7, apoptotic cells with numerous PRB7 binding signals including large aggregates were gradually generated during 4 days of culture. This finding is the first direct evidence of the generation and accumulation of β-sheet-rich prion protein in ScN2a cells. Interestingly, in these apoptotic cells, SAF32-staining granules were distinct from PRB7-binding aggregates, suggesting that SAF32-binding PrP does not have a PRB7-recognizing β-sheet structure, whereas PRB7-binding PrP may not have the N-terminal octarepeat region of PrP. After ScN2a cells were cultured in the presence of PRB7 or SAF32 for 3 days, PK-treated cell lysate was immunoblotted by 6D11 to examine the inhibitory effects of PRB7 IgG on the generation/accumulation of PrP^{Sc}. Surprisingly, PRB7 IgG had no influence, whereas SAF32 strongly inhibited the generation/accumulation of PrP^{res}.

Thus, this study reports the first establishment of a human IgG antibody recognizing β-form PrP but not α-form PrP and the use of this antibody to provide direct evidence of the *de novo* generation and conversion of β-sheet-rich PrP in prion-infected cells. PRB7 IgG can be a powerful tool to purify the β-form PrP generated *de novo* and demonstrate its biochemical basis and significance to elucidate structural evidence of prion infectivity and neurotoxicity.

EXPERIMENTAL PROCEDURES

Reagents and Antibodies—The pQE30 vector and *Escherichia coli* (M15) were obtained from Qiagen. The 6D11 antibody was purchased from Signet. A silver stain II kit was from Wako. Phenylmethylsulfonyl fluoride (PMSF) and anti-β-tubulin (I) antibody were purchased from Sigma. Recombinant anti-PrP Fab HuM-P, HuM-D18, HuM-D13, HuM-R72, and HuM-R1 were purchased from Inpro Biotechnology. GAHu/Fab/Bio was purchased from Nordic Immunology Inc. Horseradish peroxidase (HRP)-conjugated anti-goat mouse IgG, alkaline phosphatase-conjugated goat anti-mouse IgG, and goat anti-human IgG Fc-HRP were purchased from Jackson ImmunoResearch Laboratories. HisTrap™ HP, the anti-His tag antibody, and HiTrap™ Protein A HP were from GE Healthcare. The mouse anti-E tag monoclonal antibody, HRP-conjugated anti-E tag mAb, the anti-E tag antibody-Sepharose column, and the anti-M13 monoclonal antibody were purchased from Amersham Biosciences. The 3,3′,5,5′-tetramethylbenzidine solution was from Calbiochem. SAF32 was purchased from SPI Bio (Ann Arbor, MI). Control human IgG/κ was purchased from Bethyl Laboratories. Alkaline phosphatase-conjugated streptavidin and HRP-conjugated streptavidin were purchased from Vector Laboratories. The Dye Terminator Cycle Sequencing FS Ready Reaction kit was from Applied Biosystems. NheI, BstApI, ApaI, BsaWI, BbsI, and HindIII were obtained from New England Biolabs (Ipswich, MA). T4 DNA ligase was obtained from Takara Bio Inc. Opti-MEM, the SuperScript™ First-Strand Synthesis System, pcDNA3.1™(−) mycHisA, pcDNA3.1(−) Zeo, the FreeStyle™ MAX reagent, Annexin V-Alexa Fluor 568, Alexa Fluor 488-labeled anti-human IgG, Alexa Fluor 546-labeled anti-mouse IgG, and Alexa Fluor 488-succinimidyl ester were obtained from Invitrogen. Anti-β-actin antibody was purchased from Abcam. The labeling of antibody with Alexa Fluor 488 was performed according to the manufacturer's instructions. DAPI was purchased from Cambrex Bio Science.

Expression Vector—PrP expression vectors were constructed as described (11). Briefly, DNA fragments corresponding to human PrP residues 23–231 were independently amplified by polymerase chain reaction (PCR) using forward primer (5′-gcggatccaagaagcgcccgaagcctgga-3′) and back primer (5′-ccaagcttctatcagctcgatcctctctggtaata-3′) from genomic DNA of HEK293T cells. The fragments were digested with BamHI and HindIII and inserted into a pQE30 vector bearing the His tag sequence. Bovine PrP(25–242), mouse PrP(23–231), or sheep PrP(25–234) expression vectors were constructed in a similar way.

Protein Expression and Purification—Constructed histidine-tagged recombinant full-length prion protein (rPrP; amino acids 23–231) was expressed in *E. coli* (M15) and purified by HisTrap HP as described (8). Briefly, fractions containing human rPrP were diluted to a final concentration of 1 mg/ml using a 0.1 M Tris buffer (pH 8.0) containing 9 M urea and 100 mM β-mercaptoethanol. The dialyzed solution was diluted

3-fold with 0.1% (v/v) trifluoroacetic acid in water, loaded on a 10 × 150-mm WP300 C4 HPLC column (GL Sciences, Tokyo, Japan), and eluted using a gradient of 0.1% (v/v) trifluoroacetic acid in acetonitrile. Fractions containing oxidized PrP were lyophilized and stored at −20 °C as described (8).

Refolding—Refolding of rPrP was performed according to the methods of Jackson *et al.* (12). Briefly, to prepare α-form PrP, a stock solution of rPrP (1 mg/ml in 6 M GdnHCl) was dialyzed into a 10 mM sodium acetate, 10 mM Tris acetate buffer (pH 8.0). In the case of β-form PrP, rPrP was dissolved in a 100 mM dithiothreitol (DTT), 6 M GdnHCl, 10 mM Tris acetate (pH 8.0) buffer for 16 h and then dialyzed with a 10 mM sodium acetate, 1 mM DTT (pH 4.0) buffer. A half-volume of the dialysis buffer was replaced with fresh buffer, and this procedure was repeated every 12 h for a total of 10 times. Refolded proteins were stored at 4 °C. The PrP concentration was determined using a spectrophotometer, Ultrospec 2000 (Amersham Biosciences), using a molar extinction coefficient E_{280} of 56,650 M^{-1} cm^{-1}.

Circular Dichroism Spectroscopy—Circular dichroism (CD) spectra were recorded in a 0.1-cm cuvette with a J-820 spectrometer (Jasco) scanning at 20 nm/min with a bandwidth of 1 nm and data spacing of 0.5 nm. Each spectrum represents the average of five individual scans after subtracting the background spectra (8).

Atomic Force Microscopy—Atomic force microscopy images were recorded on an SPI-3800 (Seiko Instruments, Chiba, Japan) immediately after dilution of the 5.4 mg/ml solution of the β-form PrP and displaying on a fresh mica surface.

PK Digestion—Recombinant PrP (100 μg/ml) was treated with the indicated concentration of PK for 1 h at 37 °C. ScN2a cell lysates were treated with PK (final concentration, 20 μg/ml) for 30 min at 37 °C, then PMSF at a final concentration of 2 mM was added, and the mixture was centrifuged at 15,000 rpm for 45 min at 4 °C. The pellet was dissolved in a 1× SDS-PAGE sample buffer and boiled for 10 min for immunoblotting analysis.

Immunoblotting—SDS-PAGE was performed as described (13, 14). Purified PRB7 IgG was separated by 10% SDS-PAGE, and the gel was stained with the silver stain II kit.

Immunoblotting was performed as described (13, 15). Briefly, samples were added to a 2× sample buffer, boiled for 10 min, separated on a 16.5% Tricine-polyacrylamide gel, and electrotransferred onto a PVDF membrane at 150 V for 90 min using a semidry electroblotter (Sartorius, Tokyo, Japan). The membrane was blocked with 5% skim milk in PBS overnight. Specific binding of the antibody to proteins was determined by incubating the membrane for at least 1 h with the 6D11 antibody (1:4000). HRP-conjugated goat anti-mouse IgG served as a secondary antibody (1:5000). Protein signals were visualized using ECL on a LAS-1000 image analyzer (Fuji Film, Tokyo, Japan). The Tricine gel was stained with the silver stain II kit.

Phage Libraries—The human single chain Fv (scFv)-displaying M13 phage library constructed using the pCANTAB 5E (4.5-kb) phagemid vector was used in this study as described (13, 15). The peptide-displaying phage libraries (Ph.D.-12) were purchased from New England Biolabs. The Ph.D.-12 library contains linear peptides composed of 12 random amino acids.

Biopanning—Biopanning was performed as described (13–15). To isolate the antibody phage specific to β-form PrP, the scFv phage library (1×10^{12} pfu/50 μl) was preabsorbed with α-form PrP (5 μg) coating an immunotube under the conditions of a folding buffer (pH 8.0). One hour later, unbound phages were collected and added to a β-form PrP (5 μg)-coated immunotube under the conditions of a folding buffer (pH 4.0). After 1 h of incubation at room temperature, the unbound phages were discarded by washing the immunotubes seven times with folding buffer (pH 4) containing 0.1% Tween 20. The bound phages were then eluted with 0.1 M glycine-HCl (pH 2.2), immediately neutralized with 1 M Tris-HCl (pH 9.1), and amplified by infection with log phase *E. coli* strain TG1 cells. The phages and soluble scFv were prepared as described (13–15). To isolate peptide phage to PRB7 IgG, unrelated control human IgG/κ and PRB7 IgG were separately immobilized on polystyrene 96-well microplates (300 ng/50 μl/well). The Ph.D.-12 phage library (4×10^{11} transforming units) was preabsorbed on a plate immobilized by unrelated control human IgG/κ. The phages were incubated at room temperature for 1 h with immobilized PRB7 IgG, and the binding phages were eluted with 0.1 M glycine-HCl (pH 2.2). The eluate was immediately neutralized with 1.0 M Tris-HCl (pH 9.1) and amplified by infecting ER2738.

Preparation of Aβ42 Conformers—Aβ42 conformers were prepared as described (14, 16). Synthetic Aβ42 peptides (purity 90–95% by mass spectrum; Peptide Institute Inc., Osaka, Japan) were solubilized in 1,1,1,3,3,3-hexafluoro-2-propanol (Wako, Tokyo, Japan) at a concentration of 1 mg/ml (222 μM) and separated into aliquots in microcentrifuge tubes. Immediately prior to use, the 1,1,1,3,3,3-hexafluoro-2-propanol-treated Aβ42 was dissolved in dimethyl sulfoxide (Wako) to 4 mg/ml (888 μM) and diluted with a 20 mM phosphate buffer (pH 7.4) to a concentration of 40 μM.

ELISA—ELISA was performed as described (13–15). Briefly, a microtiter plate (Nunc, Denmark) was coated with refolded PrP (100 ng/50 μl/well) and anti-His tag mAb (80 ng/40 μl/well) for 1 h at room temperature. BSA (0.25%)/PBS was used as blocking buffer. BSA (0.25%)/PBS containing 0.1% Tween 20 was used as washing buffer. Anti-PrP Fab (HuM-P, HuM-D18, HuM-D13, HuM-R72, or HuM-R1; 1:500) (17–19) was detected by the biotinylated anti-Fab antibody (1:1000; 50 μl/well) in combination with alkaline phosphatase-conjugated streptavidin. Soluble PRB7 scFv (200 ng/40 μl/well) was detected by the anti-E tag antibody in combination with alkaline phosphatase-conjugated goat anti-mouse IgG (1:1000). PRB7 IgG (0–1 μg/ml; 50 μl/well) was detected by goat anti-human Fc-HRP (1:2000; 50 μl/well). SAF32 (0.1 μg/ml; 50 μl/well) was detected by HRP-conjugated goat anti-mouse IgG (1:5000; 50 μl/well). Antibody phage clones (5×10^{11} transforming units/40 μl) were incubated with the indicated refolded PrP (200 ng/40 μl) in a folding buffer (pH 4.0 or 8.0) and then captured on wells coated with an anti-His tag mAb. The bound phage was detected using a biotinylated anti-M13 mAb (1:1000) followed by the addition of alkaline phosphatase-conjugated streptavidin (1:1000). In the case of sandwich ELISA, PRB7 or control human IgG/κ (100 ng/25 μl) was incubated with human β-form PrP (100 ng/25 μl) in a pH 4.0 folding

buffer for 1 h and then added into wells precoated with an anti-PrP mAb, SAF32 or 6D11 (100 ng/50 μl). After treatment with a blocking and washing solution, the bound antibody was detected using an HRP-conjugated anti-human IgG (1:5000). In the case of the alkaline phosphatase development system, absorbance was measured at 405 nm during incubation with 50 μl of a *p*-nitrophenyl phosphate, 10% diethanolamine solution by use of a microplate reader (NJ-2300, PerkinElmer, Tokyo). In the case of the HRP development system, the plates were incubated with 50 μl of 3,3′,5,5′-tetramethylbenzidine solution for 3 min at room temperature in the dark. After addition of 50 μl of 1 N HCl, absorbance was measured at 450 nm using the EnSpire 2300 Multilabel Reader (PerkinElmer Life Sciences).

To perform the epitope mapping of PRB7 IgG, a microtiter plate was coated with 50 ng/50 μl/well PRB7 IgG or control IgG/κ for 1 h at 4 °C. After blocking the plates with 0.25% BSA, PBS, Ph.D.-12 phage clones (50 μl/well of 1×10^{11} virions/ml) were added to each well followed by incubation with a biotinylated anti-M13 monoclonal antibody (1:2000) in combination with HRP-conjugated streptavidin (1:2000).

DNA Sequencing—The nucleotide sequences of the scFv genes were identified using the Dye Terminator Cycle Sequencing FS Ready Reaction kit with primers pCANTAB5-S1 (5′-CAACGTGAAAAAATTATTATTCGC-3′) and pCANTAB5-S6 (5′-GTAAATGAATTTTCTGTATGAGG-3′).

Size Exclusion Chromatography (SEC)—SEC (7.8 × 300-mm TSK-GEL G3000SWXL HPLC column, Tosoh Corp., Tokyo, Japan) was performed as described (20). The column was equilibrated with buffer A (20 mM sodium acetate (pH 8.0), 200 mM NaCl, 1 M urea, 0.02% sodium azide) for α-form PrP or buffer B (20 mM sodium acetate (pH 4.0), 200 mM NaCl, 1 M urea, 0.02% sodium azide) for β-form PrP and used at room temperature with a flow rate of 1 ml/min (20).

Construction of PRB7 IgG Expression Vectors—DNA primers were synthesized by Hokkaido System Science Co. (Sapporo, Japan). The outline is presented in supplemental Figs. S1 and S2. The heavy-chain leader sequence (Vhls; HAVT20) (21), heavy-chain variable gene (Vh), light-chain leader sequence (Vlls) (13), and light-chain variable gene (Vl) of PRB7 were amplified by PCR (22) using Vhls forward primer 1 (5′-AAAAATCTAGAGCTAGCGATGGCATGCCCTGGCTTCCTGTGGGCACTTGTGATCTCC-3′), Vhls back primer (5′-AAAAAGCAACAGCTGCACCTCAGCCATGGAAAATTCAAGACAGGTGGAGATCACAAGTGCC-3′), Vh forward primer (5′-GAGGTGCAGCTGTTGCAG-3′), Vh back primer (5′-AAAAAGGGCCCTTGGTGGATGAGGAGACGGTGAC-3′), Vlls forward primer (5′-AAAAAGCTAGCGATGGAAACCCCAGCGCAGCTTCTCTTCC-3′), Vlls back primer (5′-AAAAATCCGGTGGTTGGGAGCCAGAGTAGCAGGAGGAAGAGAAGCTGCGC-3′), Vl forward primer (5′-AAAAAACCGGAGACATCGTGATGACCCAG-3′), and Vl back primer (5′-AAAAAGAAGACAGATGGTGCAGCCACAGTACGTTTAATCTCCAGTCGGT-3′). The Vhls fragment contains the NheI site at the 5′ terminus and the BstApI site at the 3′-terminus. The Vh fragment contains the BstApI site at the 5′ terminus and the ApaI site at the 3′ terminus. The Vlls fragment contains the NheI site at the 5′ terminus and the BsaWI site at the 3′ terminus. The Vl fragment contains the BasWI site at the 5′ terminus and the BbsI site at the 3′ terminus. The constant region of human immunoglobulin heavy chain 1 (IGHC1) and human immunoglobulin κ-chain (IGKC) (21) was amplified from cDNA of peripheral blood lymphocytes by PCR using IGHC1 forward primer (5′-TCCACCAAGGGCCC-3′), IGHC1 back primer (5′-AAGCTTCGGAGACAGGGAGAG-3′), IGKC forward primer (5′-ACTGTGGCTGCACCATC-3′), and IGKC back primer (5′-AAGCTTCTAACACTCTCCCCTGTTG-3′). The IGHC1 fragment contains the ApaI site at the 5′ terminus and the HindIII site at the 3′ terminus. The IGKC fragment contains the BbsI site at the 5′ terminus and the HindIII site at the 3′ terminus. The cDNA was prepared using the SuperScript First-Strand Synthesis System.

For the construction of the PRB7 IGHC1 expression vector, the Vhls fragment and the Vh fragment were digested with BstApI. These two fragments were ligated with T4 DNA ligase. The ligated sample was amplified by PCR using Vhls forward primer 2 (5′-AAAAATCTAGAGCTAGCGATGGCATG-3′) and the Vh back primer. This amplified fragment and the IGHC1 fragment were digested with ApaI, ligated, and amplified by PCR using Vhls forward primer 2 and the IGHC1 back primer. This amplified fragment was digested with NheI and HindIII and inserted into a pcDNA3.1(−) mycHisA vector.

For the construction of the PRB7 IGHC1 expression vector, the Vlls fragment and the Vl fragment were digested with BsaWI, ligated with T4 DNA ligase, and amplified by PCR using the Vlls forward primer and the Vl back primer. This amplified fragment and the IGKC fragment were digested with BbsI, ligated, and amplified by PCR using the Vlls forward primer and the IGKC back primer. The amplified fragment was digested with NheI and HindIII and inserted into a pcDNA3.1(−) Zeo vector.

Protein Expression and Purification of PRB7 IgG—FreeStyle 293F cells (Invitrogen; 1×10^6 cells/ml) were co-transfected with an equimolar mixture (final total DNA concentration, 1 μg/ml) of a heavy-chain expression vector and a light-chain expression vector with the FreeStyle MAX reagent (final concentration, 1 μl/ml) according to the manufacturer's instructions (23). Transfections were performed in 500-μl cultures as described above. One week later, the supernatant was harvested from the culture by centrifugation. PRB7 IgG was purified using HiTrap Protein A HP according to the manufacturer's instructions (13).

Computer Simulation of PrPs—The computer simulation was performed on the basis of the NMR structure of the human PrP (amino acids 124–227; Protein Data Bank code 1QM0) (24) using PyMOL software. Human IgG was simulated by use of Molecular Operating Environment™ (MOE, Version 2009.10) (supplemental Fig. S3).

Cell culture—ScN2a cells, N2a58 cells overexpressing mouse PrP (a genotype with codons 108L and 189T), FF32 cells, or N2aL1 cells were used. FF32 cells were cloned from F3 cells (an N2a58 cell line infected with a prion Fukuoka-1 strain derived from mouse brain infected with a brain of a Gerstmann-Straüssler-Scheinker syndrome patient) or N2aL1 cells (an N2a58 cell line infected with the 22L strain derived from mouse brain infected with scrapie) as described previously (25, 26). All cells were cultured in Opti-MEM containing 10% fetal bovine serum and penicillin-streptomycin at 37 °C in 5% CO_2. Cells (5×10^4 cells/well in a 24-well plate) were cultured in the

absence or presence of varying concentrations of PRB7 IgG, SAF32, control human IgG/κ antibodies (azide-free), Alexa Fluor 488-PRB7 IgG, or Alexa Fluor 488-control human IgG/κ antibodies (azide-free) at 37 °C on 24-well microplates (Iwaki Glass Co.) (27).

Immunostaining—Immunostaining was performed as described (28–30). Briefly, cells were cultured in an Advanced TC™ glass bottom cell culture dish (Greiner Bio-One, Germany). Three days later, cells were fixed with 4% paraformaldehyde for 20 min at room temperature and then washed with PBS. In the case of staining of β-actin or β-tubulin, cells were fixed with cold methanol for 30 min at −20 °C. Fixed cells were permeated with 0.2% saponin, PBS for 20 min; washed with PBS; and blocked with 3% BSA, PBS for 30 min at room temperature. These cells were incubated with SAF32 (5 μg/ml) for 1 h at room temperature in 1.5% BSA, 0.1% saponin, PBS. After washing with PBS, cells were incubated with DAPI (1:2000), Alexa Fluor 488-labeled anti-human IgG (1:2000), and Alexa Fluor 546-labeled anti-mouse IgG (1:2000) diluted in 1.5% BSA, 0.1% saponin, PBS for 1 h at room temperature. For Annexin V staining, non-fixed cells were incubated with Annexin V-Alexa Fluor 568 (1:100) diluted in an annexin binding buffer (10 mM HEPES, 140 mM NaCl, and 2.5 mM $CaCl_2$, pH 7.4) for 30 min at room temperature. To stain the denatured prion, permeated cells were treated with 6 M GdnHCl for 10–30 min at room temperature.

Confocal Microscopy Analysis—Fluorescence images were acquired using a Zeiss LSM 700 confocal laser microscope (Carl Zeiss, Tokyo, Japan). Orthogonal projections were generated from z-stacks, and profile projections were generated using Zeiss LSM software (Carl Zeiss).

RESULTS

Characterization of Recombinant Human Full-length PrP—PrP was prepared using recombinant prion protein as described (8). CD analysis showed the typical characteristics of the α-form of PrP with a structure rich in α-helical content and of the β-form with a β-sheet rich structure, respectively (Fig. 1*A*) (31). Atomic force microscopy of the β-form of PrP displayed a round shaped particle, showing the formation of globular structures with an apparent diameter (horizontal) of ~47 nm and an apparent height of ~1.6 nm (Fig. 1*B*). α-Form PrP was digested completely with 2 μg/ml PK, whereas β-form PrP showed resistant fragments at 8 μg/ml PK treatment (Fig. 1*C*). D18 antibody recognizes the epitope 133–157 of α-form PrP but not β-form PrP (17–19). In accordance with this finding, D18 did not bind to this β-form PrP. D13 (epitope 96–106 of PrP), R72 (epitope 152–163 of PrP), or the P antibody (epitope 96–105 of PrP) did not distinguish the structural difference between the α-form and the β-form of PrP (Fig. 1*D*) (17–19).

Biopanning against β-Form of PrP—The immunotube for biopanning was prepared by coating the tube with β-form PrP (5 μg) dissolved in pH 4.0 solution. The phage solution (10^{12} pfu/50 μl) preabsorbed to α-form PrP was added to the β-form PrP-coated immunotube under the condition of a folding buffer (pH 4.0). After two rounds of biopanning selection, ELISA was performed under the pH 8.0 condition to determine the binding activity to α-form PrP because α-form PrP was folded under the pH 8.0 condition. On the other hand, the binding activity to β-form PrP was examined under the pH 4.0 condition. A total of 384 clones were isolated and tested for binding activity to antigen by ELISA. Two scFv phage clones, designated as PRB7 and PRB30, were selected to be specific for the β-form of PrP without binding activity to the α-form of PrP (Fig. 2*A*).

PBR7 and PBR30 scFv were then purified by affinity column and tested for their binding specificity using a pH 7.3 buffer (Fig. 2*B*). Both scFv clearly showed marked binding activity to the β-form but not the α-form of PrP or an unrelated negative control protein, His-tagged human TIM-3.

It is possible that the pH of the experimental condition influences the conformation of PrPs or scFv, resulting in gain or loss of the binding activity. Therefore, to examine more carefully the effects of the pH condition on PrP/scFv binding, after plates had been coated with folded PrP at the corresponding pH, ELISA was performed for 1 h under either pH 4.0 or 8.0. The almost identical results indicated that the binding of PRB7 and PRB30 was specific to β-form but not α-form PrP (supplemental Fig. S4). In concert with the conformation specificity of these clones, they showed no binding activity to the SDS-denatured form of full-length PrP, indicating that both scFv are specific to the conformational structures of β-form PrP (data not shown). It was confirmed that PRB7 reacted with the β-form PrP in native PAGE (supplemental Fig. S5).

Gene Usage of PRB7 and PRB30—The amino acid sequence of scFv clones was deduced from the DNA sequence. The complementarity-determining regions (CDR1–CDR3) and the frame regions (FR1–FR4) were assigned by searching the IMGT/V-QUEST database. PRB7 and PRB30 have unique sequences in both Vh and Vl genes, respectively (Fig. 3*C*).

PRB7 and PRB30 Recognize Conformation of β-Form PrP Monomer and Oligomer but Not That of α-Form PrP—PrP was fractionated by size exclusion chromatography. The α-form of PrP was eluted as a single peak (α-form PrP fraction 1) at an elution time of 11.8 min in a running buffer at pH 5.0 (20 mM sodium acetate, 200 mM sodium chloride, 1 M urea, 0.02% azide). For the β-form of PrP, the sample was resolved as two peaks at an elution time of 7.5 (β-form PrP fraction 1) and 12.6 min (β-form PrP fraction 2) in a running buffer at pH 4.0 (20 mM sodium acetate, 200 mM sodium chloride, 1 M urea, 0.02% azide) (Fig. 4*A*). α-Form PrP fraction 1 exhibited a typical α-helical spectrum, whereas β-form PrP fraction 1 and β-form PrP fraction 2 exhibited a typical β-sheet structure in CD analysis (Fig. 4*B*).

To test the binding activity of these fractions to PRB7 and PRB30, each fraction was immobilized on microtiter plates. As shown in Fig. 4*C*, PRB7 or PRB30 bound to β-form PrP fraction 1 as well as β-form PrP fraction 2. Both scFv showed no binding to α-form PrP, amyloid β42 monomer peptide, IL-18, or BSA. In contrast, the authentic mouse anti-PrP monoclonal antibody SAF32 bound to every PrP fraction irrespectively of their conformations. Its binding epitope is located at the N-terminal octarepeat region of the α-form of PrP (27). Unrelated scFv (RE51) gave no binding reactions to any coated proteins.

PRB7 IgG and Its Binding Specificity—IgG form of PBR7 scFv was constructed to endow PRB7 scFv with molecular stability. PRB7 IgG purified with a Protein A column was analyzed by

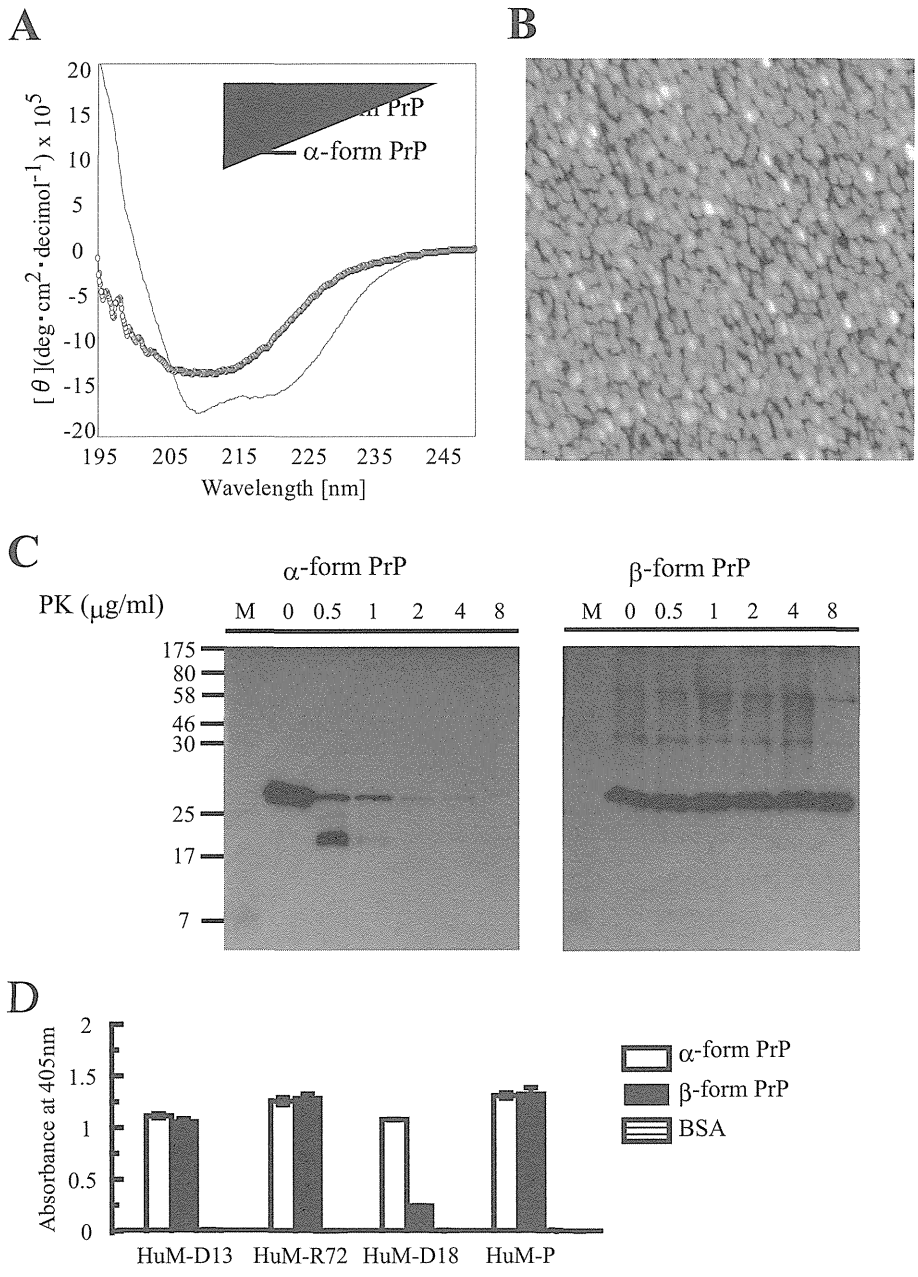

FIGURE 1. **Characterization of human full-length prion protein refolded *in vitro*.** Refolding was performed according to the protocol of Jackson *et al.* (12). *A*, CD spectra for the protein refolded at pH 8.0 (*line*; α-form PrP) and the protein refolded at pH 4.0 (*open circle*; β-form PrP). A double minimum at 222 and 208 nm or a minimum at ~215 nm is characteristic of an α-helical structure or β-sheet structure, respectively (26). *B*, atomic force microscopy image of β-form PrP. *C*, limited PK digestion of β-form PrP. α-Form PrP or β-form PrP (1 μg) was incubated with varying concentrations (0–8 μg/ml) of PK for 30 min at 37 °C. PrP was detected by immunoblot analysis with the 6D11 antibody. *D*, reactivity of α-form PrP or β-form PrP with HuM anti-PrP antibodies (17–19). Region 133–157 recognized by the anti-PrP Fab antibody (D18) is cryptic in β-PrP. Data represent the mean values ±S.D. *deg*, degrees.

SDS-PAGE, which indicated that the IgG form associated with a γ- and κ-chain with a disulfide bond (Fig. 5*A*). The PRB7 IgG showed an identical binding specificity to PRB7 scFv with specific binding to β-form PrP but not α-form PrP, whereas SAF32 bound equally to β-form PrP and α-form PrP (Fig. 5*B*). Furthermore, PRB7 IgG showed no binding activity to Aβ42 soluble form, prefibril oligomers, or fibril forms (Fig. 5*B*).

Epitope Mapping of PBR7 IgG—Epitope mapping was performed using a linear peptide-displaying phage library (Ph.D.-12) and a circular peptide-displaying phage library (Ph.D.-C7C). PRB7 IgG-binding clones (pepPRB7-14) were isolated from Ph.D.-12 among 70 clones tested, whereas no clone was selected from Ph.D.-C7C. The binding activity of PBR7 IgG to the pepPRB7-14 clone is shown in Fig. 6*A*.

The amino acid sequence homology search using ClustalW version 3.1 indicated that the pepPRB7-14 peptide motif had weak homology to 124–136, particularly 128–132 of the human full-length prion protein, suggesting that PRB7 IgG recognizes this epitope (Fig. 6*B*). The 124–136 region is depicted in *red* in the PyMOL display of the NMR structure of the α-form of PrP (24).

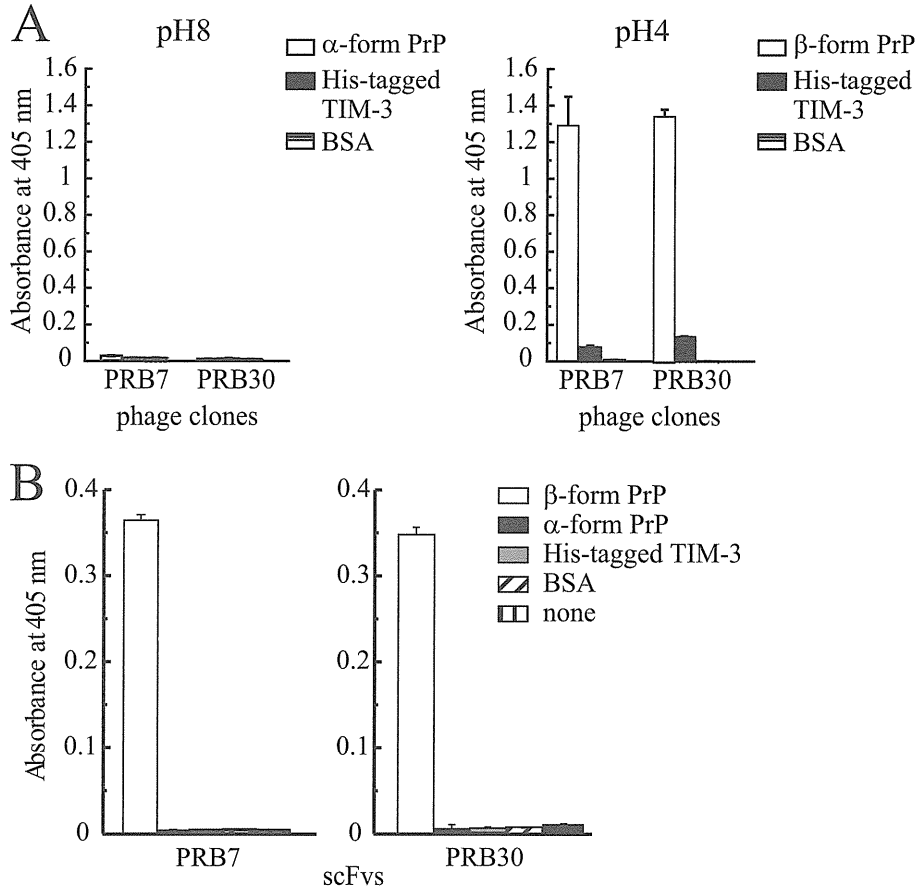

FIGURE 2. **Binding specificity of β-form PrP-selected scFv phage clones by ELISA.** *A*, phage clones (PRB7 or PRB30; 5×10^{11} transforming units/40 μl) were incubated with the indicated antigens (200 ng/40 μl) in a pH 8.0 or 4.0 folding buffer for 1 h and then added to wells coated with an anti-His tag mAb. The bound phage was detected using a biotinylated anti-M13 monoclonal antibody (1:1000) followed by the addition of alkaline phosphatase-conjugated streptavidin (1:1000) as described under "Experimental Procedures." His-tagged TIM-3 or BSA was used as a control protein. *B*, soluble PRB7 or PRB30 scFv antibody (1 μg/200 μl) was added to the indicated antigen-coated ELISA plates (200 ng/40 μl/well) using pH 7.3 binding buffer. The bound scFv antibodies were detected using a biotinylated anti-E tag monoclonal antibody (1:1000) followed by the addition of alkaline phosphatase-conjugated streptavidin (1:1000). Data represent the mean values ±S.D.

A

		FR1	CDR1	FR2	CDR2	FR3
PRB7	scFv	EVQLLQSAG-GVVQPGRSLSLSCAAS	GFTSRTYA----	MHWVRQAPGKGLEWVAV	VSPDGSDR--	FYGDLVK-GRFTISRDNSRSTLSLQMDSLRVEDTAVYYC
PRB30	scFv	QVQLQESGG-GLVKPGGSLRLSCAAS	GFMFGSYT----	MHWVRQAPGKELEWVSS	ISSWSNPI--	HYADSVK-GRFIISRDNAQNSLYLQINSLRVDDTAVYYC

		CDR3	FR4
PRB7	scFv	ARGASS------SSRNHFAIDV	WGQGTLVTVSS
PRB30	scFv	ARPPSTDHDYRSGSVGF-FDN	WGQGTLVTASS

B

		FR1	CDR1	FR2	CDR2	FR3
PRB7	scFv	DIVMTQSPSTLSASVGDRVTITCRAS	QSISR-W------	LAWYQQKPGQPPRLLIS	GAS--------	SRATGIP-DRFSGSGSGTDFTLTISRLEPEDFAVYYC
PRB30	scFv	EIALTQSPGTLSLSPGERATLSCRAS	QSVSSSY------	LAWYQQKPGQAPRLLIY	DAS--------	NRASGIP-ARFSGRGSGTDFTLTITSLEPEDFAVYYC

		CDR3	FR4
PRB7	scFv	QQYGSSPGT	FGQGTRLEIKR
PRB30	scFv	QQRSNWPPT	FGQGTKVEIKR

C

	Heavy chain			Light chain	
clone#	V	D	J	V	J
PRB7	IGHV3-30*04	IGHD2-15*01	IGHJ6*02	IGKV3-20*01	IGKJ5*01
PRB30	IGHV3-21*01	IGHD3-3*01	IGHJ4*02	IGKV3-11*01	IGKJ1*01

FIGURE 3. **Amino acid sequence analysis of identified scFv specific to β-PrP.** *A*, Vh domains. *B*, Vl domains. *C*, the germ line gene usage of anti-β-PrP scFv. Given are the names of the gene segments according to the IMGT database. *, other possibilities: IGHJ5*01 and IGHJ4*01 (highest number of consecutive identical nucleotides) or IGHJ4*01 (shorter alignment but highest percentage of identity).

PRB7 IgG Recognizes Common β-Conformation of PrP Shared by Human, Bovine, Sheep, and Mouse—Recombinant PrP of human, bovine, mouse, or sheep was folded according to the protocol of Jackson *et al.* (12). The CD spectrum of each PrP preparation is shown in Fig. 7*A*. When the binding activity of PRB7 IgG to these PrPs was examined by ELISA, PRB7 IgG exclusively

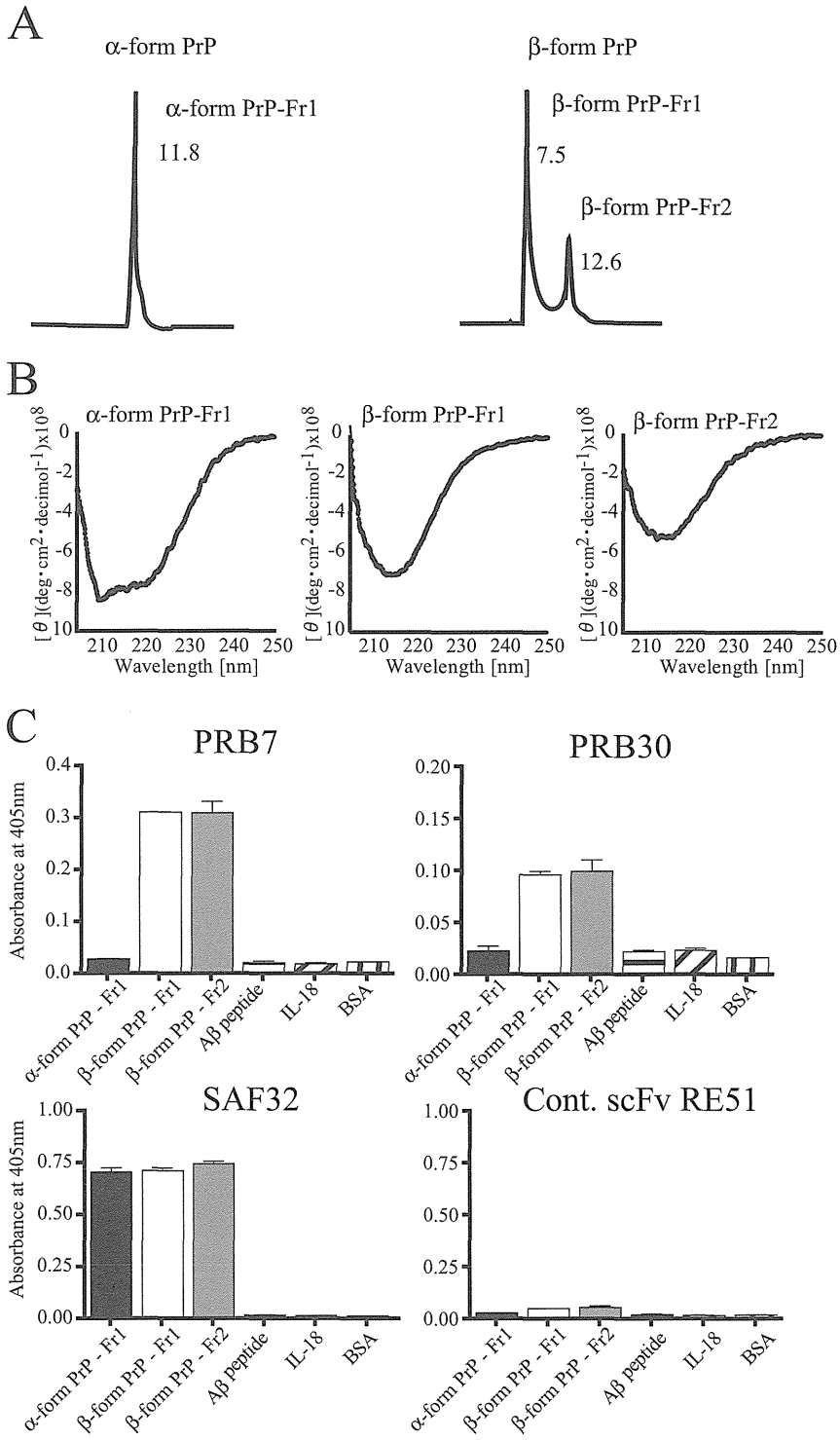

FIGURE 4. **PRB7 and PRB30 scFv recognize β-form PrP monomer and oligomer fractionated by SEC.** *A*, SEC profile of α-form PrP (*left*) and β-form PrP (*right*). α-Form PrP or β-form PrP was eluted with a running buffer in the presence of 1 M urea at pH 5.5 or a running buffer in the presence of 1 M urea at pH 4.0, respectively. *B*, CD spectra of SEC-fractionated samples. The CD signals at wavelengths below 200 nm (not shown) are distorted as a result of absorption by urea. *C*, the scFv antibodies were added to wells coated with SEC-fractionated samples. PRB7 or PRB30 scFv antibody recognized β-form PrP-Fr1 and β-form PrP-Fr2 but not α-form PrP-Fr1, amyloid β42 peptide, or IL-18. Unrelated scFv (RE51) showed no binding activity to any of these proteins. Data represent the mean values ±S.D. *Cont.*, control; *deg*, degrees.

bound to the β-form of PrP but not the α-form of PrP (Fig. 7*B*, *left panel*). This reactivity is shared by human, bovine, sheep, and mouse PrP. SAF32 strongly recognized both forms of every species without any discrimination (Fig. 7*B*, *right panel*).

β-Form PrPs Are Generated and Accumulate de Novo in Prion-infected ScN2a Cells—PRB7 recognizes the fine structure of the conformation of PrP and does not stain ScN2a cells fixed with paraformaldehyde. Furthermore, PRB7 IgG hardly stained

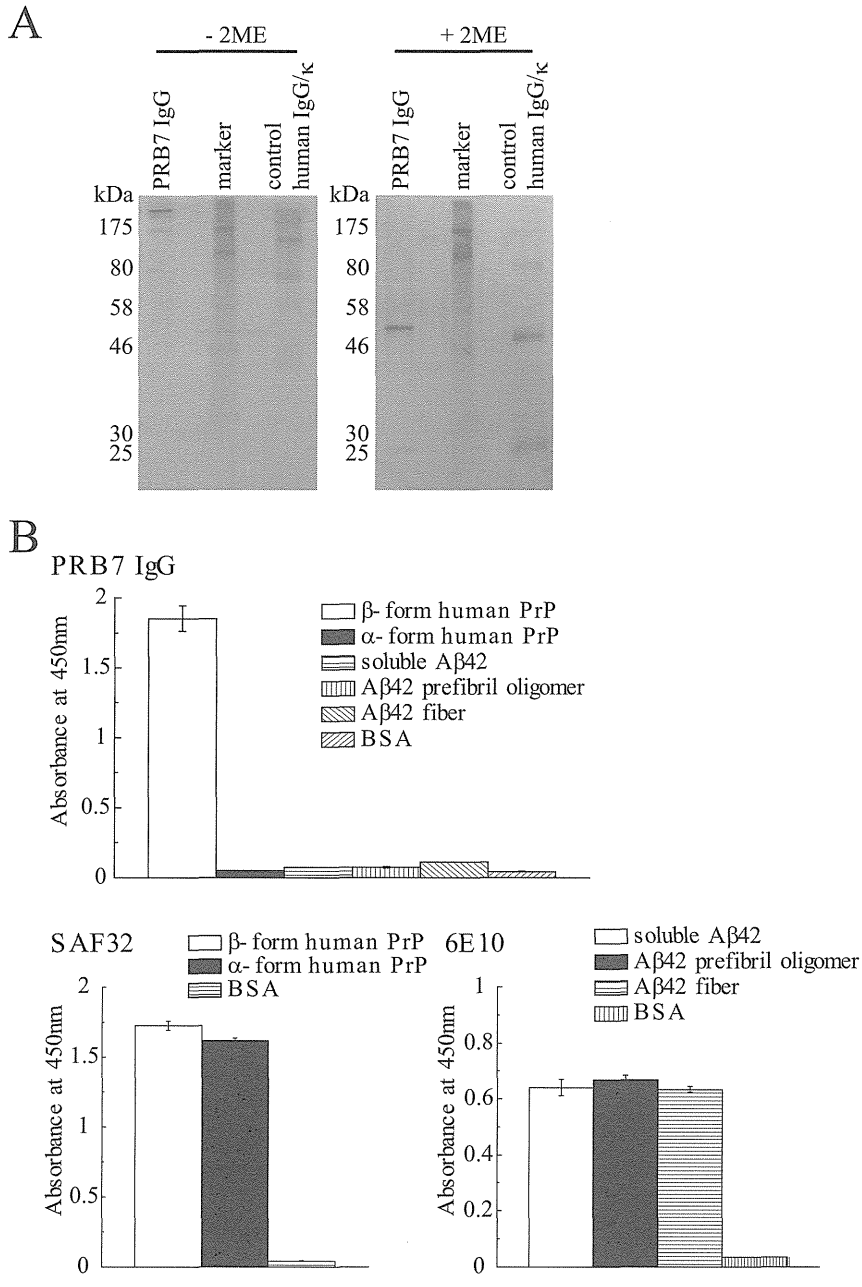

FIGURE 5. **Characterization of PRB7 IgG antibody.** *A*, SDS-PAGE of PRB7 IgG. Protein A column-purified PRB7 IgG (300 ng) was separated by 10% SDS-PAGE under reducing or non-reducing condition and detected by silver staining. *B*, PrP conformers (50 ng/50 μl/well) were detected by PRB7 IgG or SAF32 (0.5 μg/ml). Aβ42 conformers (50 ng/50 μl/well) were tested for binding reactivity to PRB7 IgG or 6E10 (mouse anti-Aβ42 antibody) as described under "Experimental Procedures." *2ME*, 2-mercaptoethanol. Data represent the mean values ±S.D.

cell surfaces of non-fixed ScN2a cells, suggesting scarce existence of β-form PrP on the cell surface (supplemental Fig. S6). Therefore, to examine the generation of β-form PrP in prion-infected cells, prion-infected ScN2a cells were cultured in the presence of PRB7 IgG or SAF32. Three days later, cells were fixed with paraformaldehyde. After permeation with saponin, cells were stained with Alexa Fluor 488-anti-human IgG to detect the complex of PRB7 IgG-PrP or SAF32-PrP (Fig. 8*A*). Control cells, N2a58 non-infected cells, or ScN2a cells in the presence of normal IgG were not stained with this protocol. As the binding of normal IgG to N2a58 cells or ScN2a cells was not observed by confocal microscopy or flow cytometry analysis, N2a58 cells or ScN2a cells were found to be Fcγ receptor-negative. In contrast, PRB7 IgG or SAF32 stained the cytoplasm of ScN2a but not N2a58 in a distinct image. Three staining patterns of cytoplasm were observed in ScN2a incubated with PRB7 IgG, *i.e.* cells with varying numbers of small granules, cells with very large aggregates in the cytoplasm, and cells with no staining. SAF32 stained cell surface PrP of ScN2a and N2a58 cells. When detection sensitivity of confocal laser microscopy was increased, SAF32 was detected by Alexa Fluor 546-labeled anti-mouse IgG in the cytoplasm region below the cell surface

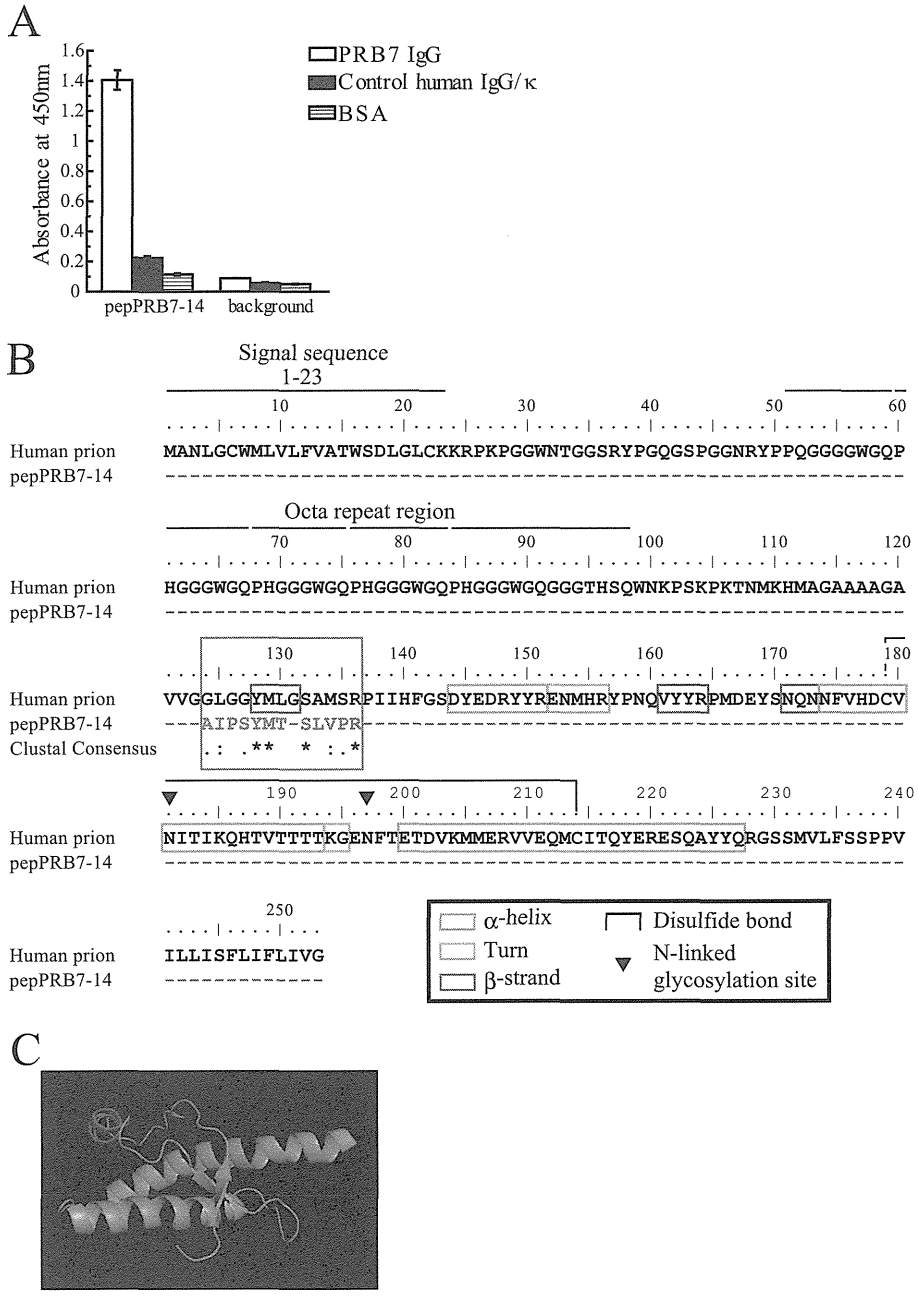

FIGURE 6. **Epitope mapping of PRB7 IgG.** *A*, peptide phage clones (50 μl/well of 1 × 10^{11} virions/ml) were incubated with PRB7 IgG (50 ng/50 μl/well). The bound peptide phage clones were detected using a biotinylated anti-M13 monoclonal antibody (1:2000) followed by HRP-conjugated streptavidin (1:2000). The pepPRB7-14 was selected from a Ph.D.-12 peptide phage library. Data represent the mean values ±S.D. *B*, amino acid sequence homology between the full-length human PrP and pepPRB7-14 motif (*red*) was searched by ClustalW. The matching region (amino acids 124–135) is depicted in the *red box*. The secondary structures are indicated by explanatory *marks* as shown in the *black box*. *C*, computer simulation model of human α-form PrP (Protein Data Bank code 1QM0). The matching region (amino acids 124–135) containing a highly homologous region (amino acids 128–132) is depicted as a *red ribbon*. PRB7 IgG does not recognize this structure of α-form PrP.

membrane of ScN2a. When these cells were fixed with methanol and stained with anti-β-actin or anti-β-tubulin antibody, the PRB7 IgG-bound aggregates were evident in ScN2a cells cultured with PRB7 IgG (Fig. 8*B*). The details of the PRB7-staining features of ScN2a cells cultured with PRB7 IgG are investigated in Fig. 9. About 4000 cells were classified on the basis of the number of stained granules. Cells without granules amounted to 71%, and those with one granule amounted to 16%. Cells with more than 10 granules amounted to 0.6%. Among these cells, 0.4% of cells with very large aggregates in the cytoplasm were particularly conspicuous. Although ScN2a cells with enormous aggregates in the entire cytoplasm were stained with anti-β-actin (Fig. 8*B*), these cells were analyzed for the existence of nuclei over the perpendicular axis using serial images taken by confocal microscopy, and traces of nuclei were detected by DAPI (Fig. 10*A*, *white arrow*). Annexin V weakly

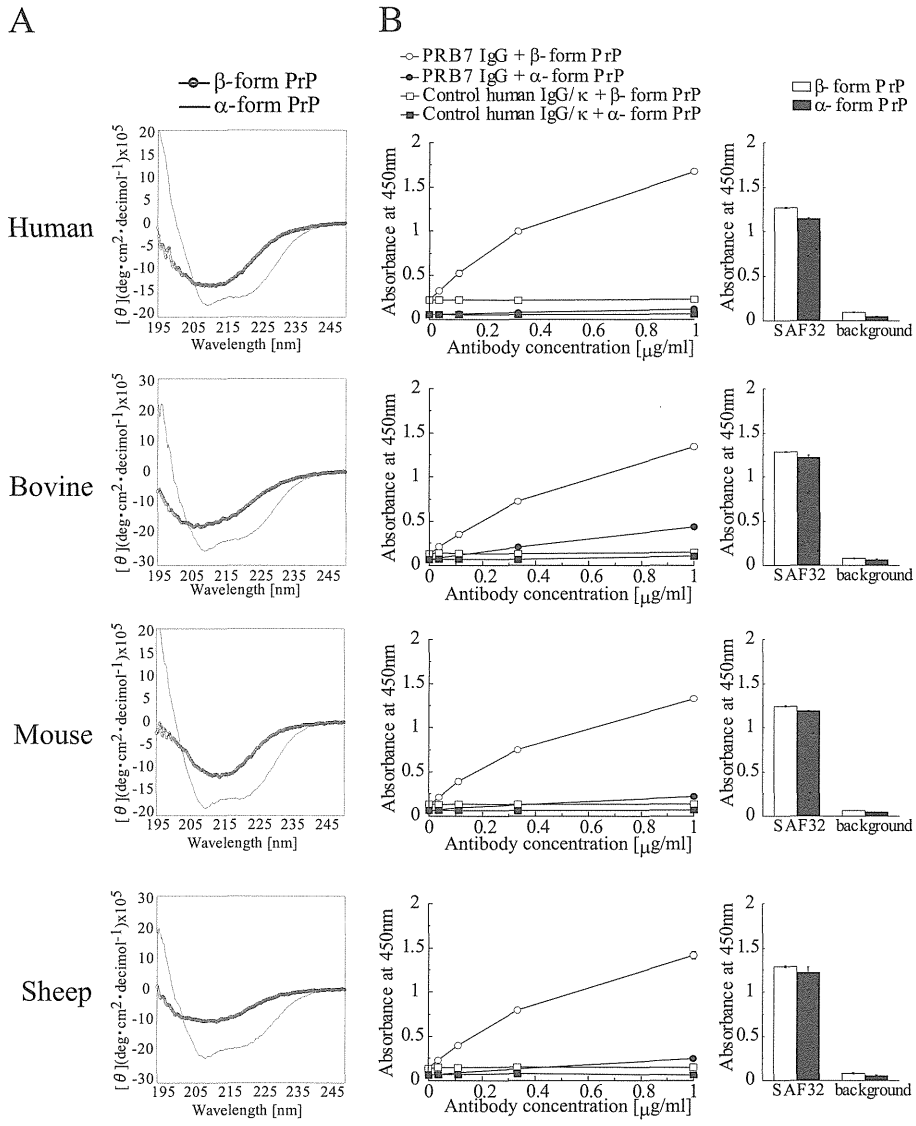

FIGURE 7. **Binding specificity of PRB7 IgG by ELISA analysis.** *A*, CD spectra of α-form PrP and β-form PrP. Recombinant PrP was refolded as described under "Experimental Procedures." *B*, ELISA of PRB7 IgG antibodies binding to PrP. *Left panel*, PRB7 IgG (ranging from 0 to 1 μg/ml) was incubated with PrP-coated plates (100 ng/50 μl/well). Normal human IgG was used as a control. The secondary antibody was HRP-conjugated anti-human IgG (1:5000 dilution). *Right panel*, SAF32 (0.1 μg/ml) equally binds to both α-form PrP and β-form PrP (100 ng/50 μl/well). The background was determined using HRP-conjugated anti-human IgG alone. Data represent the mean values ±S.D. deg, degrees.

stained these cells with enormous aggregates, indicating that these cells had undergone apoptosis, whereas Annexin V did not stain cells that were strongly DAPI-positive (Fig. 10*A*). When cells with enormous aggregates were stained with SAF32 in addition to PRB7, however, this staining image observed from the perpendicular axis was not completely merged in PRB7- and SAF32-staining PrP (Fig. 10*B*, *white arrow*). A magnified image of the B region of Fig. 10*B* indicated that PRB7 IgG stained very large tangled fibrillary aggregates, whereas SAF32 appeared to independently stain distinctive tiny granules dispersed in the entire cytoplasm (Fig. 10*C*, *right panel*). Similarly, in the case of ScN2a cells with clear DAPI-positive nuclei and numerous small PRB7 IgG-bound granules, SAF32 stained another part of the cytoplasm distinct from PRB7 IgG (Fig. 10*C*, *left panel*). These cells with a number of tiny PRB7-positive granules were clearly stained with Annexin V, indicating that they had undergone apoptosis (Fig. 10*D*). These results suggested that PRB7 IgG-bound granules were antibody complexes with N-terminal region-deleted PrP. To confirm whether PRB7 IgG-bound complexes were composed of PrP, ScN2a cells cultured with Alexa Fluor 488-labeled PRB7 IgG were denatured with 6 M GdnHCl and stained with an another anti-PrP antibody, 6D11, which recognizes the epitope located at 93–109 of PrP (32). PrP is sandwiched with PRB7 IgG and 6D11 in ELISA (supplemental Fig. S7). As shown in Fig. 10*E*, SAF32 or 6D11 did not visualize tiny aggregates in the cytoplasm of non-denatured ScN2a cells, whereas PRB7 IgG stained large aggregates in the same cells (Fig. 10*E*, *panels 1* and *2*). In the case of GdnHCl-denatured ScN2a cells, SAF32 or 6D11 stained numerous tiny aggregates in the cytoplasm (Fig. 10*E*,

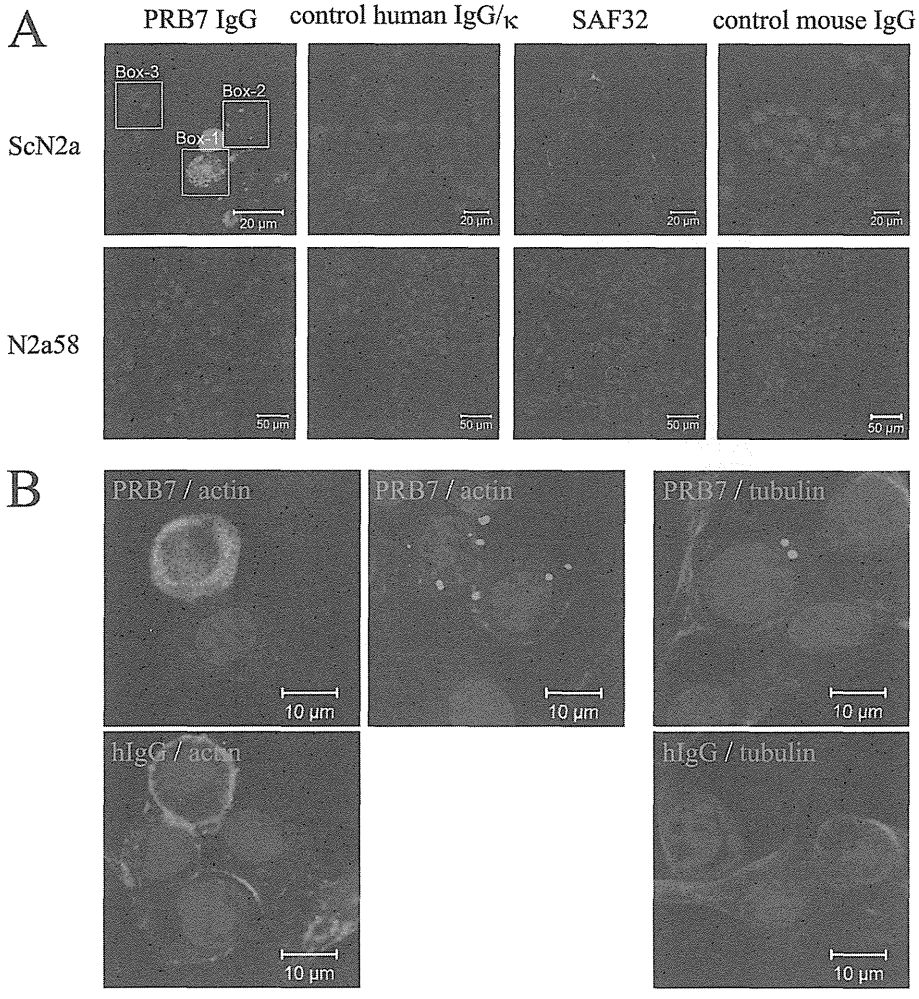

FIGURE 8. **β-Form PrPs are generated and accumulate *de novo* in prion-infected ScN2a cells.** *A*, ScN2a or N2a58 cells were cultured in the absence or presence of PRB7 IgG, SAF32, control human IgG/κ, or control mouse IgG (5 μg/ml) in 10% FBS, Opti-MEM. Three days later, cells were fixed with paraformaldehyde and permeated for staining with Alexa Fluor 488-labeled anti-human IgG (*green*), Alexa Fluor 546-labeled anti-mouse IgG (*red*), or DAPI (*blue*) as described under "Experimental Procedures." Each *box* indicates a representative staining pattern. *Box 1*, *Box 2*, and *Box 3* show Large/many granules, a few tiny granules, or no granules stained with PRB7 IgG, respectively. *B*, ScN2a cells cultured in the presence of PRB7 IgG or control human IgG/κ (*hIgG*) (*green*) as described in *A* were fixed with methanol and stained with anti-β-actin antibody (*red*), anti-β-tubulin antibody (*red*), or DAPI (*blue*) as described under "Experimental Procedures."

panels 3 and *5*). PRB7 IgG showed a distinct image in the same cells (Fig. 10*E*, *panel 4*) where two kinds of staining images were observed, *i.e.* non-merged and merged aggregates with PRB7 IgG and 6D11 (Fig. 10*E*, *panels 6* and *8*). Fig. 10*E*, *panel 7*, shows a three-dimensional image of Fig. 10*E*, *panel 6*. These results suggested that there were not only PRB7 IgG-bound aggregates that had lost SAF32 and 6D11 epitopes but also 6D11 epitope-retaining aggregates bound with PRB7 IgG.

PRB7 IgG Showed No Inhibitory Activity on Accumulation of PrP^{res} in ScN2a Cells—ScN2a cells were cultured in the absence or presence of PRB7 IgG or SAF32. Four days later, cell extracts were prepared in the presence of varying concentrations of PK. The resultant PrP^{res} was evaluated by immunoblotting with 6D11. As shown in Fig. 11, SAF32 strongly inhibited the accumulation of PrP^{res}, indicating the internalization of SAF32 antibody in the cytoplasm after binding to cell surface PrP (Fig. 8). In contrast to the strong inhibitory activity of SAF32, PRB7 IgG showed no effects on the accumulation of PrP^{res}, similar to the effects of control IgG. These results indicated that SAF32 but not PRB7 IgG blocked prion or PrP^{Sc}, preventing the generation of β-form PrP.

DISCUSSION

A number of studies showed that prions generate and accumulate PrP^{Sc}, which shows resistance to PK degradation. It is postulated that PrP^{Sc} converts PrP^{C} to PrP^{Sc} by its templating activity. PrP^{Sc} was purified as a multimer or aggregates. The protease-resistant core of PrP^{Sc}, designated PrP27–30, polymerizes into an amyloid. Many purified amyloids have been found to have a β-pleated sheet structure. From these findings, it is believed that prion or PrP^{Sc} may have a β-sheet-rich structure (3, 5).

Is PrP^{Sc} a β-form PrP? Antibodies should be a powerful tool to solve this question. Despite the insufficient biochemical characterization of PrP^{Sc}, many attempts have been made to establish antibodies with fine specificity using mice immunized

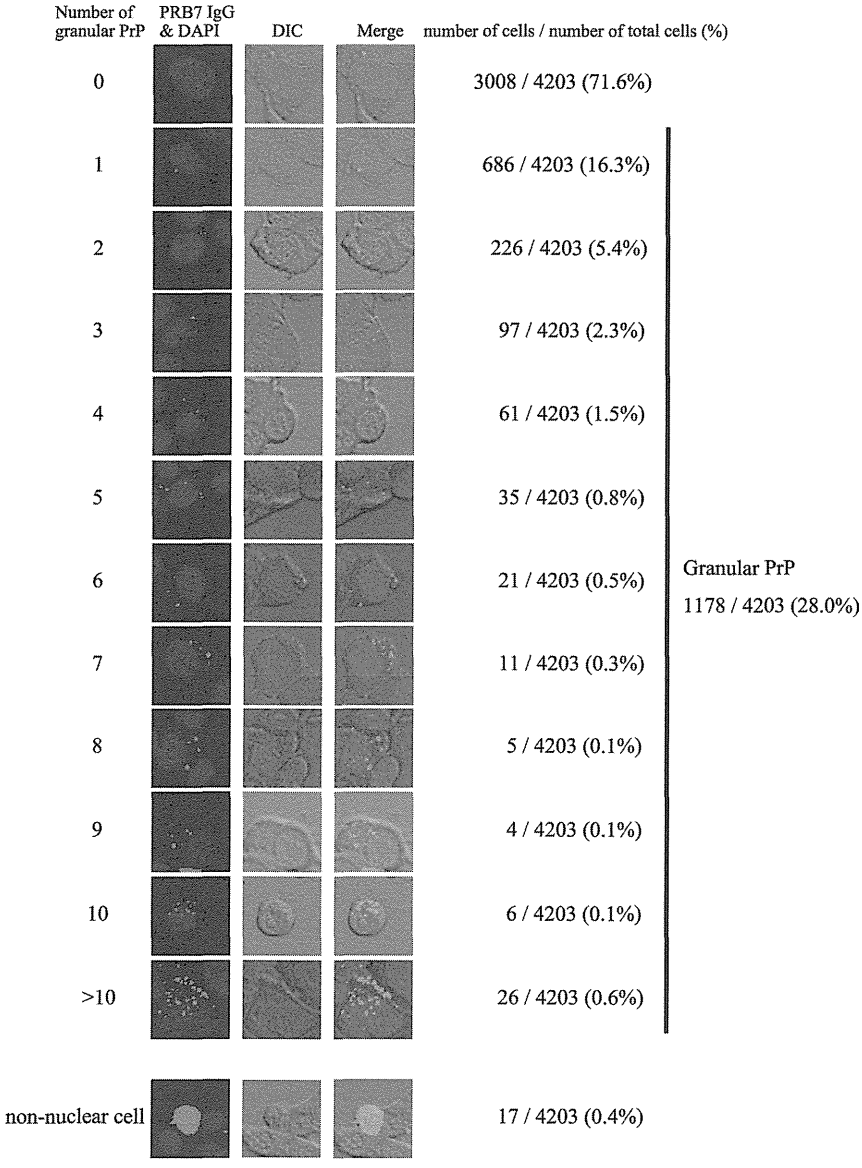

FIGURE 9. **Distribution pattern of PRB7 IgG-positive granules in ScN2a cells cultured with PRB7 IgG.** Cells were stained with PRB7 IgG or DAPI as described in Fig. 8. A total of 4203 cells were classified by the number of granules in the cytoplasm (positive cells/total cells observed). *DIC*, differential interference contrast.

with partially purified PrP^{Sc} from prion-infected cells or brain extracts (6, 10, 33–42). However, most antibodies were specific to PrP^{C} or cross-reactive to both PrP^{C} and PrP^{Sc} but not monospecific to PrP^{Sc}, although more recently a PrP^{Sc}-specific murine IgG1 antibody, W261, has been established (10). However, even in this situation, PrP conformation-specific antibodies have not been developed.

In this study, using conformation-defined recombinant β-form PrP and an antibody-displaying phage library, we established a β-form PrP-specific human IgG1 antibody, PRB7 IgG. This antibody does not recognize generic oligomer or aggregate forms of unrelated proteins in accordance with the binding activity of PRB7 or PRB30 scFv. PRB7 IgG is the first human IgG antibody specifically binding to β-form PrP monomer and oligomers but not α-form PrP. It is suggested that PRB7 IgG recognizes the epitope 128–132 of β-form human PrP. PRB7 IgG is equally cross-reactive to the β-form of bovine, sheep, and mouse PrP.

As PRB7 IgG does not recognize paraformaldehyde-fixed or denatured PrP molecules, we simply observed the ScN2a cells cultured with PRB7 IgG. We have demonstrated here that prion-infected ScN2a cells specifically internalized PRB7 IgG and accumulated the PrP granules bound with PRB7 IgG in the cytoplasm (Fig. 8). This is the first direct demonstration that β-form PrP was generated and accumulated in prion-infected cells in the physiological condition. Because neither ScN2a nor N2a58 cells were stained with normal IgG as assessed by confocal microscopy or flow cytometry, these cells were Fcγ receptor-negative. Nevertheless, ScN2a cells internalized PRB7 IgG, suggesting that complexes of β-form PrP targeted by PRB7 IgG

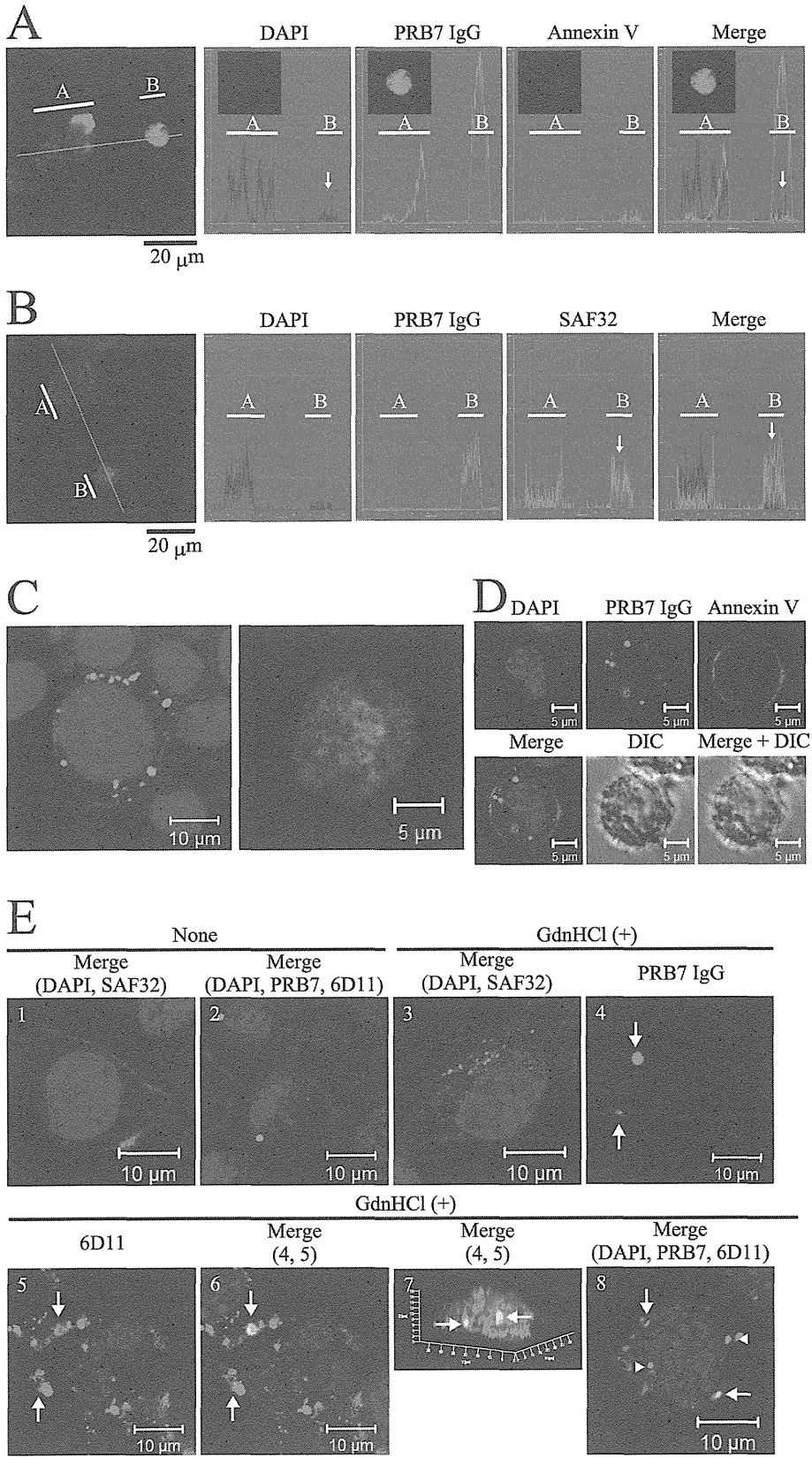

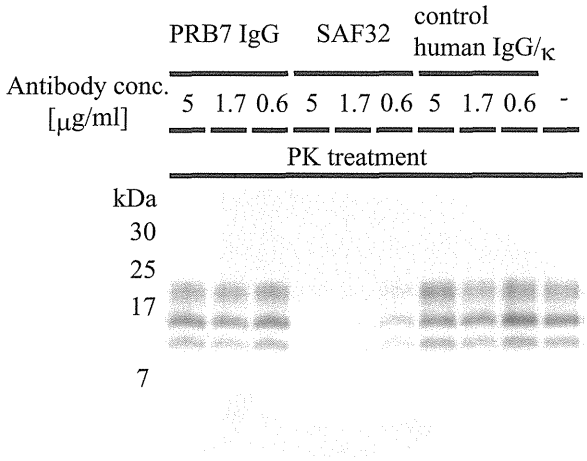

FIGURE 11. **Effect of PRB7 IgG on accumulation of PrP^{res}.** ScN2a cells were cultured with PRB7 IgG, SAF32, or control human IgG/κ antibodies ranging from 0 to 5 μg/ml for 4 days at 37 °C. In the case of "−", ScN2a was cultured without antibody for 4 days at 37 °C. Cell lysates were treated with PK (final concentration (*conc.*), 20 μg/ml) as described under "Experimental Procedures." Lysates were separated on a 16.5% Tricine-polyacrylamide gel and immunoblotted with 6D11 antibody followed by HRP-conjugated anti-goat mouse IgG as described under "Experimental Procedures."

localizing on the cell surface were endocytosed into the cytoplasm (29). If this β-form PrP corresponds to PrP^{Sc}, this observation is in accordance with the finding that PrP^{Sc} was generated on a lipid raft on the cell surface (43). When ScN2a cells were cultured with PRB7 IgG, they gradually generated an increasing number of tiny PRB7-binding granules in the cytoplasm. Among them, about 0.4% of cells had enormous aggregates in the cytoplasm. Vertically severed images of these cells show traces of nuclei in cells that were weakly stained with Annexin V, indicating that they had undergone apoptosis (Fig. 10*A*). These findings suggested that an enormous aggregate resulted from the fusion of many tiny β-form granules primarily endocytosed from the cell surface but was not the result of β-form PrP propagation in the cytoplasm.

SAF32 bound tiny granules dispersed in the cytoplasm that were distinct from large aggregates stained with PRB7 IgG (Fig. 10*C*). These results suggested first that PRB7-positive β-form PrPs lost or hid the N-terminal octarepeat region to which SAF32 bound and second that granules stained with SAF32 were not generated from β-form PrP.

It was suggested that PrP^{C}-PrP^{Sc} conversion, which is physiologically prevented by an energy barrier, may be a spontaneous stochastic event favored by mutations in the *PRNP* gene or acquired by infection with exogenous PrP^{Sc}. Accordingly, it is conceivable that GdnHCl treatment of cells additively induces the conformational conversion of PrP, leading to the formation of aggregates in experiments that immunohistologically attempted to show granules of PrP^{Sc} in the cytoplasm (8). It is noted that when ScN2a cells were stained with SAF32 or 6D11 with a denaturing pretreatment by 6 M GdnHCl numerous tiny PrP granules became visible in the cytoplasm, and their images were quite distinct from those of PRB7-staining aggregates. Our results indicated that apoptotic cells showed two distinct types of PrP granules in the cytoplasm: one was SAF32-negative and PRB7 IgG-positive granules (N-terminal region-deleted; β-form PrP), and the other was PRB7 IgG-negative and SAF32-positive granules (full-length PrP lacking a β-sheet-rich conformation) (Fig. 10*E*). Related studies have reported that PK-sensitive PrP^{Sc} was contained in prion aggregates (44) and more recently that there is heterogeneity in PrP^{Sc} conformers including small soluble PrP aggregates (6). Regarding the requirement of full-length PrP for prion activity, the answer is not consistent: *i.e.* Prusiner *et al.* (50) reported that the purified PK-digested PrP27–30 was not infectious, whereas Anaya *et al.* (45) have recently reported that small infectious PrP^{res} aggregates were recovered in the absence of strong *in vitro* denaturing treatments from prion-infected cultured cells. On the other hand, using an anti-aggregated PrP IgM antibody, 15B3, Biasini *et al.* (6, 47) reported the successful purification of pathological full-length prion aggregates, and Cronier *et al.* (46) found that PK-sensitive PrP^{Sc} was involved in prion aggregates. Our findings in Fig. 10 suggest that PrP composed of tiny aggregates visualized with SAF32 or 6D11 after 6 M GdnHCl treatment of cells may be a full-length PrP with α-conformation.

To examine the influence of PRB7 IgG on the templating activity of β-form PrP to accumulate PrP^{Sc}, ScN2a cells were cultured in the presence of PRB7 IgG or SAF32, and their PK-treated cell lysates were immunoblotted with 6D11 to evaluate the amount of PrP^{res}. Surprisingly, PRB7 IgG had no effect,

FIGURE 10. **ScN2a cells exhibit PRB7 IgG-positive aggregates under apoptosis.** Cells were stained with PRB7 IgG (*green*), SAF32 (*red*), or DAPI (*blue*) as described in Fig. 8. *A*, ScN2a cells with very large aggregates in the cytoplasm underwent apoptosis. ScN2a cells cultured with PRB7 IgG were incubated with Annexin V (*red*) followed by fixing, permeation, and staining with anti-human IgG or DAPI as described under "Experimental Procedures." Orthogonal projections of serial confocal sections are shown by histograms alongside one z-section taken from the middle of the cell (as indicated by the *red guidelines*). *White bar A* or *B* indicates the range of the guideline. The *white arrow* in the *B* range indicates the pattern of a huge aggregate-bearing ScN2a cell. *Scale bar*, 20 μm. *B*, very large aggregates in the cytoplasm are PrP. ScN2a cells cultured with PRB7 IgG were fixed, permeated, and stained with SAF32 followed by secondary antibody staining with Alexa Fluor 488-labeled anti-human IgG or Alexa Fluor 546-labeled anti-mouse IgG. Orthogonal projections of serial confocal sections are shown by histograms alongside one z-section taken from the middle of the cell (as indicated by the *red guidelines*). *White bar A* or *B* indicates the range of the guideline. The *white arrow* in the *B* range indicates the pattern of a huge aggregate-bearing ScN2a cell. *C*, PRB7 IgG-positive images do not merge with SAF32-positive images. *Left image*, prion-infected ScN2a cells containing a number of small PRB7 IgG-bound granules. SAF32 stained the entire region of cytoplasm except PRB7 IgG-bound granules. *Right image*, prion-infected ScN2a cells containing large tangled fibrillary aggregates stained with PRB7 IgG. A number of tiny granules were stained with SAF32 independently of PRB7 IgG-positive aggregates. *D*, ScN2a cells with a number of PRB7 IgG-positive granules around nuclei underwent apoptosis. ScN2a cells cultured with PRB7 IgG were incubated with Annexin V followed by fixing, permeation, and staining with anti-human IgG or DAPI as described in *A*. *E*, ScN2a cells cultured with Alexa Fluor 488-PRB7 IgG were fixed, permeated, treated with (+) or without (−) 6 M GdnHCl, and stained with 6D11 (epitope 93–109 of PrP (32)). *Panel 1* is an image merged with DAPI and SAF32 staining of non-treated ScN2a cells. *Panel 2* is an image merged with DAPI, PRB7 IgG, and 6D11 staining of non-treated ScN2a cells. *Panels 3–8* show the images of 6 M GdnHCl-treated ScN2a cells. *Panels 4–7* show images of an identical cell. *Panel 3* is an image merged with DAPI and SAF32 staining. *Panel 4* is an image stained with Alexa Fluor 488-PRB7 IgG. *Panel 5* is an image stained with 6D11. *Panel 6* is an image merged with PRB7 IgG and 6D11 staining. *Panel 7* is a three-dimensional image of *panel 6*. *Panel 8* shows a cell containing heterogeneous PRB7 IgG-bound aggregates merged with (*white arrow*) or without (*white arrowhead*) 6D11 staining in the presence of numerous tiny aggregates stained with 6D11 in the cytoplasm. Staining was performed as described under "Experimental Procedures." *DIC*, differential interference contrast.